Electron interaction cross sections for CF_3I, C_2F_4, and CF_x (x=1-3) radicals

I. Rozum,* P. Limão-Vieira,† S. Eden, and J. Tennyson‡
Department of Physics and Astronomy, University College London, Gower St., London WC1E 6BT, UK

N. J. Mason
Centre of Molecular and Optical Sciences, The Open University, Milton Keynes MK7 6AA, UK

The supply of absolute electron–impact cross sections for molecular targets and radicals is extremely important for developing plasma reactors and testing different types of etching gases. Current demand for such models is high as the industry aims to replace traditional plasma processing gases with less polluting species. New theoretical electron impact cross sections at typical etching plasma energies (sub 10 eV) are presented for the CF_x (x=1-3) active radical species in a form suitable for plasma modeling. The available experimental and theoretical data are summarised for two potential feed gases, CF_3I and C_2F_4. This data covers recommended cross sections for electron scattering (total, excitation, momentum transfer and elastic integral), electron impact dissociation and dissociative electron attachment, wherever possible. Numerical values are given as tables in the paper and are also placed in the electronic archive.

PACS numbers: 34.80.-i, 52.20, 52.77.-j
Keywords: electron molecule collisions, cross sections, resonances, electronic excitation, dissociative electron attachment, ionisation, technological plasmas.

Contents

List of Tables

List of Figures

*Present address: Department of Chemistry, University of Manchester, Manchester M13 9PL, UK
†Also at Departamento de Física, CEFITEC, FCT - Universidade Nova de Lisboa, Quinta da Torre, P–2829-516, Caparica, Portugal
‡j.tennyson@ucl.ac.uk

1. INTRODUCTION

The unique properties of the plasma phase provide powerful solutions to a number of industrial and manufacturing problems. In semi-conductor etching, plasmas can give access to chemically active species (ions and radicals) from a relatively inert feed gas. Furthermore, sufficient energy can be deposited onto the etch surface by ion bombardment to accelerate chemical reactions without exposing the sample to damaging temperatures [1]. Today the industry relies upon the development of plasma technology to produce progressively more detailed and compact systems while also meeting increasingly severe environmental legislation.

Technological plasmas are partially ionised, partially dissociated gases. They contain electrons, atomic ions, molecular ions and neutrals. The neutral species include molecules of the original gas, products of chemical reactions in the plasma or on the sample surface, and fragments of the parent gas dissociated by electronic, ionic and photonic collisions. The density of free radicals in a fluorocarbon plasma typically used in semiconductor processing is of the order of 10^{14} cm^{-3}, compared with ion concentrations of around 10^{10} cm^{-3} [2]. Therefore, free radicals such as CF, CF_2 and CF_3 are expected to play a key role in the etching process and the evolution of the plasma. Indeed, recent studies show that the concentration of CF_x radicals has a significant effect on the behaviour of fluorocarbon plasmas citecha01,cha03.

Despite the establishment of plasma etching technology at the foundation of one of the world's most profitable and progressive manufacturing industries, most plasma processing development is based on empirical techniques. The processes for optimisation and innovation of the current technology can thus be considered somewhat fortuitous and inefficient. The current demand for redevelopment is particularly high in order to meet the environmental targets set by the Kyoto Protocol [3]. Accordingly, major investment has been directed towards experiments for *in situ* plasma diagnosis [4] and the development of large scale computer models to simulate the conditions within a plasma processing cell [5]. Models which aim to represent technological plasmas accurately depend upon precise cross sectional data for all the possible electron interactions with the constituent neutral species and ions.

SiO_2 plasma etching is conventionally carried out using CF_4, C_2F_6, C_3F_8, CHF_3 and c-C_4F_8. These species have high global warming potentials (GWP) because they absorb in the infrared window (800 cm^{-1} - 1300 cm^{-1}), and have very long residence times in the Earth's atmosphere [6]. CF_4, for example, remains for up to 50 000 years [7]. The current generation of plasma reactors release a large proportion of feed gas into the atmosphere. Therefore an effective way to reduce harmful emissions is to introduce new etchant gases whose properties lessen global warming effects.

CF_3I and C_2F_4 have attracted considerable interest as possible alternative feed gases. CF_3I is expected to have a lifetime in the atmosphere of less than 2 days due to UV photolysis [8] while that of C_2F_4 is estimated to be 1.9 days due to reactions with OH radicals [9]. Both processes produce water soluble compounds which are short lived in the atmosphere due to the ten day hydrological cycle. Therefore, terrestrial ground level CF_3I and C_2F_4 emissions cannot not contribute significantly to global warming. Within a plasma reactor, it is possible to produce high yields of CF_3 radicals (as well as CF_2 and CF) by direct electron impact dissociation of CF_3I along the C–I bond [10, 11]. Similarly, due to the weak C=C bond, C_2F_4 can be readily dissociated into CF_2 fragments by electron impact [12]. It has recently been proposed that by using a combination of CF_3I and C_2F_4, highly efficient and selective SiO_2 etching can be achieved by independently controlling the etch rate and $(CF_2)_n$ polymerization on the sample surface through the relative concentration of CF_3 and CF_2 radicals [13].

Research carried out over the last decades into plasma processing gases and their products has largely focused upon fundamental properties of the relevant molecules and ions and their interactions with electrons for energies below a few hundreds of eV. Cross sections for electron scattering, electron impact ionization and electron impact dissociation have been obtained for a number of feed gases. Recently, efforts have been made to compile reliable data for the molecules and radicals listed in table I (CF_3I, C_2F_4, CF, CF_2 and CF_3). The reviews from Christophorou and Olthoff [14, 15] on CF_3I and the theoretical calculations on radicals CF, CF_2 and CF_3 from Rozum *et al* [16–18] and Rozum and Tennyson [19] on the integral elastic and excitation, and differential electron scattering cross sections for energies below 10 eV, provide a better understanding of the relevant electron-induced processes involving the above molecules. However, there is still a lack of data on electron interactions for these species [15]. In particular, no absolute cross sections for electron attachment and dissociation are available in the literature for many species from table I. These parameters are of major significance since they determine the ionization balance within the plasma and thus key plasma properties such as the electron energy distribu-

TABLE I: Data on the electron collision processes cross sections. Data on CF_x (x=1-3) radicals is given for the energies typical in low-energy plasmas (< 10 eV).

Cross section	CF	CF_2	CF_3	CF_3I	C_2F_4
Total	a	a	a	b	e
Momentum transfer	a	a	a	b,c	f
Elastic electron scattering	a	a	a	c	f
Dissociative attachment	a*	a*	a	b	–
Electronic excitation	a	a	a	d	g
Dissociation into neutrals	a*	a*	–	d	–

a. this work; b. [14]; c. [23]; d. [24]; e. [25]; f. [26]; g. [27]; * estimated values (see text for details).

tion. Cross sections for dissociative electron attachment (DEA) and dissociation into neutrals also provide information about radical and negative ion densities [20]. Experimental data for the CF_x radicals exists only for electron impact ionization [21, 22]. Since CF_x are radical species with high reactivity it has not been possible to form beams of these molecules with which to conduct traditional electron scattering experiments. Hence, there is no experimental data on elastic or inelastic scattering from CF_x. Therefore, all the data used in modelling must be developed using theoretical techniques. This in turn is challenging since it is more difficult to accurately model the properties of radical species.

In this paper we summarize recommended cross section data for the plasma reactants CF_3I and C_2F_4, and present theoretical cross section data for the radicals CF_x (x=1-3) in a form suitable for the plasma modelling. Table I gives a summary of the data presented. All the data, corresponding to the figures shown in this paper, can be found tabulated in this paper and in the electronic archive.

2. CF_3I

Data on the elastic and inelastic electron scattering from CF_3I, including an extensive study of its electronic state spectroscopy using both photon absorption and electron scattering techniques, have been obtained from a series of measurements [24, 28–30] as well as by means of recent theoretical calculations [23].

The high-resolution VUV photoabsorption spectrum recorded by Mason *et al* [24] is characterised by three distinct regions. The first electronic excitation region is a very weak continuum arising from dipole forbidden transitions centred about 4.7 eV. The second consists of four prominent band structures observed at around 7.4, 8.1, 9.0, and 9.8 eV respectively and contains vibrational structure from 7 to 13.5 eV. The third is a high energy region above the ionization potential showing some broader featureless peaks. The lowest region is more enhanced at lower incident energies and larger scattering angles suggesting that forbidden transitions are important in this region of the spectrum, while structures between 7.4 and 10 eV show greater differential cross sections at higher incident energies, a trend characteristic of optically allowed transitions. The broad and weak continuous $\tilde{A} \longleftarrow \tilde{X}$ absorption feature centred at 4.66 eV (266 nm) with a local maximum cross section of 6.7 x 10^{-21} m^2 is ascribed to the excitation to an antibonding orbital along the C – I bond ($n \rightarrow \sigma^*$) of the CF_3I molecule. This band has been assigned to transitions from the ground $\tilde{X}$ state to the excited $\tilde{A}$ state of the CF_3I molecule. Special attention has been devoted to the A band (350–200 nm) excitation due to the prompt dissociation along the C-I bond caused by the strong repulsive nature of the excited state. Dissociation into a ground state (fluorinated)-alkyl radical (CF_3) and a ground state I ($^2P_{2/3}$), or excited-state $I^*(^2P_{1/2})$, provides a source of radicals for etching silicon wafers in industrial plasma reactors. To a first approximation a photoabsorption cross section would be a total electronic excitation scattering cross section summed over all angles for singlet (allowed) transitions at the incident energy at which one measures the photoabsorption cross section. If the incident energy is 5 eV then this would be a limit for the total electron impact cross section for excitation of summed allowed transitions. This is an equivalent to integrating a differential cross section over all angles for a specific excitation transition(s).

The recent experimental total electron scattering cross sections [31] and the theoretical calculations of Joshipura *et al* [32] based on the Complex Optical Method (COP), have been compared with the recommended values of Christophorou and Olthoff [14]. The two sets of data [14, 31] seem to agree fairly well, especially for energies above 80 eV. However, at lower energies (e.g. 11 eV) the data of Kawada *et al* is 11% higher than the values quoted by Christophorou and Olthoff. Since there is no other recent experimental data, we chose to recommend the cross sectional values of Christophorou and Olthoff [14] (Fig. 1, Table III).

To our knowledge, no measurements of the momentum transfer and integral elastic cross section for CF_3I have been reported. The only experimental data in the literature is data derived from swarm measurements discussed by Christophorou and Olthoff [14] for very low electron energies (0.5 eV). Recently, Bettega *et al* [23] presented the first calculations on the momentum transfer and elastic integral (and differential) cross sections in the 5-30 eV electron energy range, by making use of a Schwinger multichannel method with pseudo potentials at the static exchange approximation level. These cross sections show two structures: the first below 7.5 eV and the second between 10 and 15 eV, attributable to E and A_1 symmetry representations respectively. Since no other source of momentum transfer data is available in the literature, both sets of data [14, 23] are recommended *albeit* over two different energy regions (Fig. 2, Table III). The integral elastic cross section obtained by Bettega *et al* [23] (Fig. 3, Table iV) are recommended since they are at present the only available data. Experimental data are thus urgently needed for both these processes.

The total ionization cross sections for CF_3I reported in the literature include the experimental data of Jiao *et al* [33], recommended by Christophorou and Olthoff [14], and the theoretical calculations of Joshipura *et al* [32] and Onthong *et al* [34]. The measurements on the electron impact ionization of CF_3I using a mass spectrometer, result in a total cross section reaching a value of $9.0 \pm 0.9 \times 10^{-20}$ m^2 at 70 eV [33]. The recent calculations of Onthong *et al* [34], using the Deutsch-Märk formalism, agree well with the measured cross sectional values at all impact electron energies. The maximum difference in both values of the cross section is small (about 5% at the position of the cross section maximum). The data of Joshipura *et al* [32, 35] agree well up to 70 eV, but their maximum position is shifted to higher energies when compared with the Deutsch-Märk formalism calculations. However, since Joshipura *et al's* data does not extend to lower energies, and there are no other experimental data available in the literature, the recommended ionization cross sectional values are those from Jiao *et al* [33] and Onthong and *et al* [34] (Fig. 4, Table IV).

The total (dissociative) electron attachment cross sections for CF_3I suggested by Christophorou and Olthoff [14] from an analysis of the available measured cross section data are shown in Fig. 5 and Table IV). There are to date no data reported on the total dissociation (into neutrals) cross sections, however the VUV photoabsorption studies of Mason *et al* [24] show evidence of a dissociative character of band *A*.

3. C_2F_4

Data on the elastic and inelastic electron scattering from C_2F_4, including an extensive study of its spectroscopy using both photon absorption and electron scattering techniques, have recently been obtained in a comprehensive series of measurements [27].

The tetrafuoroethylene photoabsorption cross section studies of Eden *et al* [27], in the energy range 3.9 - 10.8 eV, assigned the electronic excitation mainly in the C = C antibonding orbitals. The first transition, observed by electron energy loss spectroscopy measurements, was assigned to a $\pi \rightarrow \pi^*$, singlet $\rightarrow$ triplet transition at 4.79 eV. Several other states are excited at higher energies showing strong coupling with vibrational excitation. Furthermore, in the $\pi \rightarrow \pi^*$, singlet $\rightarrow$ singlet excited state and in the ionic ground state, they observed particularly strong motion of two different modes of CF_2 stretching coupled to a C = C stretching series. These experiments may be compared with the recent work of Nakumura *et al* [36] who calculated the excitation energies of the lowest singlet states of C_2F_4 – unfortunately there is poor agreement with the recent experimental data. The experimental results are, however, consistent with the dominant dissociation pathways of C_2F_4 being the formation of CF_2 radicals, as is required for its use as a possible replacement feed gas for dry silicon etching.

Jiang *et al* [37] calculated the total cross sections for electron scattering by C_2F_4, in the electron energy range 30-3000 eV, by means of an additivity rule (AR) and energy-dependent geometric additivity rule (EGAR) approaches. Their cross sections agree well for high electron energies; at low and intermediate energies (30–100 eV) the cross sections show large differences. Joshipura *et al* [32] performed calculations, based on the Complex Optical Method (COP), in the 50-2000 eV region. The only experimental data on the total cross section for C_2F_4 available is the recent paper of Szmytkowski *et al* [25]. Good agreement is found with the theory at higher energies and we therefore recommend to use this experimental data for the low energy cross sections.

To date there is a lack of experimental data on both elastic and inelastic scattering cross sections from C_2F_4. However, Winstead and Mckoy [26] have reported detailed theoretical analysis for elastic and inelastic collisions of low-energy electrons with C_2F_4. The momentum transfer (Fig. 6, Table V) and integral elastic electron scattering (Fig. 7, Table V) cross sections were obtained by means of a Schwinger multichannel (SMC) variational method. Electron impact excitation cross sections were also reported for the *T* and *V* states arising from the $\pi \rightarrow \pi^*$ transition (the lowest with an excitation energy at 4.48 eV), as well as for eight other low-lying excited states [26]. This data, together with electron transport properties and swarm analysis, was subsequently used by Yoshida *et al* [38] to derive a self-consistent set of electron impact cross sections for C_2F_4.

There have been no reported experimental measurements of the total ionization cross section of C_2F_4, but recently Joshipura *et al* [32] calculated the total ionization cross section using their independent atom approximation (Fig. 8, Table V). The values are likely to be valid at high energies (> 100 eV) but may be less reliable close to threshold. An experimental measurements of this cross section is therefore urgently required.

Dissociative electron attachment has been studied in the energy range 0 – 15 eV and reveals a variety of anionic fragments but F^- is the dominant ion [39]. Total electron attachment rate constants have also been reported by Goyette *et al* [40] in the 4 – 100 eV energy range. At present there are no data reported for the total dissociation (into neutrals) cross section.

It must therefore be concluded that at present the data base C_2F_4 is far from satisfactory and that considerable effort, both experimentally and theoretically, is required if the data necessary for modelling C_2F_4 plasmas is to be collected.

4. CF

The total electron impact ionization cross section for the CF radical has been reported by Tarnovsky and Becker [21] and by Tarnovsky *et al* [22] in the energy range from 10 to 200 eV. *Ab initio* calculations which

derive the electron impact ionization cross section for the CF were performed by Bobeldijk *et al* [41] and by Deutsch *et al* [42] using the semiclassical Deutsch-Märk formalism. These calculations showed some disagreement between the measured and calculated cross sections, as the calculated cross sections are significantly higher than the experimental data. Joshipura *et al* [35] calculated the electron impact ionization cross section for the CF in the energy range 20 - 2000 eV and found that their ionization cross section is 50% higher than the experimental data reported in Huo *et al* [43].

Lee *et al* [44] studied electron–CF scattering in the energy range 1 – 500 eV using a complex optical potential to represent the electron-molecule interaction dynamics and the Schwinger variational iterative method combined with the distorted-wave approximation to solve the scattering equations. Lee *et al* [44] calculated elastic differential (DCS), integral (ICS) and momentum-transfer (MTCS) cross sections as well as total (elastic and inelastic) and absorption electron scattering cross section. They compared their results with experimental and theoretical data for electron collisions with NO (which is an isoelectronic molecule of CF). Their ICS and MTCS show a shape resonance at around 15 eV, which is well above the ionization threshold and is probably a result of their relatively crude theoretical treatment. They found very good agreement between the ICS and the MTCS for electron scattering by CF and NO for incident energies above 20 eV.

More recently Rozum *et al* [17] have used the refined R-matrix method [45] to investigate low energy (sub 10 eV) electron scattering from CF radicals. The rotationally-summed elastic DCS of Rozum and Tennyson [19] are more structured in the non-forward direction than the data of Lee *et al* [44] and predict much stronger scattering in the forward direction. The difference between two results may be attributed to the target model and a level of treatment of scattering. It is well known that electron scattering by polar molecules are dominated by dipole interactions and corresponding DCS should observe a maximum in the strongly forward direction.

The MTCS cross section for the CF radical, calculated using the *POLYDCS* program of Sanna and Gianturco [46], and corresponding data are presented in Fig. 9 and Table VI. Contrary to the results of Lee *et al* [44], who calculated MTCS in the energy region (1-500) eV, the magnitude of our cross section is higher at the scattering energy 1 eV and lower at 10 eV. The MTCS presented here show low energy structures which can be ascribed to resonances. The position of the energetically lowest lying resonant structure corresponds to the $^1\Delta$ resonance observed in the elastic integral cross section.

Low energy collisional elastic and electron impact excitation integral cross sections for CF have also been calculated in the scattering energy range 100 meV – 10 eV using the R-matrix theory. The details of these calculations have been reported elsewhere [17]. These calculations show that the electron scattering processes by the CF radical, as well as CF_2 and CF_3, are dominated by elastic processes; the total and elastic cross sections for these radicals are therefore essentially the same. Fig. 10 and Table VI present the total elastic cross section (10A), electron impact excitation cross sections for the excitation of the metastable a $^4\Sigma^-$ state (10B), dissociative A $^2\Sigma^+$ and B $^2\Delta$ states (10C) and other states C $^2\Sigma^-$ and b $^4\Pi$ (10D). All the cross section data for CF is given at its equilibrium geometry. Corresponding cross section data is presented in the electronic archive. The cross sections are rich in resonance structures which arise from the capture of the incident electron to form a temporary negative ion. These structures above about 5 eV may be artificial and attributable to pseudoresonances due to the presence of the Rydberg $^2\Sigma^+$ state and diffuse basis functions in the calculations (see [17]).

At lower energies these calculations show the presence of three shape resonances of symmetries $^3\Sigma^-$, $^1\Delta$ and $^1\Sigma^+$ with a position and width of 0.91 eV and 0.75 eV for $^1\Delta$, and 2.19 and 1.73 eV for $^1\Sigma^+$ resonance at equilibrium. The position of the $^3\Sigma^-$ resonance is very close to zero at the equilibrium bond length 2.44 a_0. As the C-F bond is stretched to 2.5 a_0 the $^3\Sigma^-$ resonance becomes bound and at 3.3 a_0 the $^1\Delta$ also becomes bound. The resonance parameters suggest that the $^1\Sigma^+$ resonance will also become bound, but only at bond lengths larger than 3.6 a_0.

Some of these resonances may lead to the dissociation of the molecule in a dissociative electron attachment which leaves stable anionic fragments. These may play a major role in plasma etching. In order to determine the fate of each resonance it is necessarily to consider the energy balance equation for the DEA process, as the incident electron may not have enough energy to dissociate a molecule. Thus, the energy balance equation for the DEA process involving the $^1\Sigma^+$ resonance of CF is

$$\Delta E = D_0(CF) - A(F) + KER \qquad (1)$$

where $D_0(CF) = 5.5 \pm 0.1$ eV [47] is the dissociation energy of CF, $A(F) = 3.4$ eV [48] is the electronic affinity of F and KER is the kinetic energy release providing momentum to the dissociative fragments. The threshold for DEA is given by $KER = 0$. Equation (1) then gives the energy $\Delta E = 2.10$ eV. The energy of an incident electron, forming the $^1\Sigma^+$ resonance, is 2.19 eV at equilibrium which may be enough to dissociate CF. The use of the reflection approximation implies that about 20% of the $^1\Sigma^+$ resonance may asymptotically dissociate to $C(^1D) + F^-(^1S)$, as the electronic affinity of F is higher than the affinity of C. The remaining 80% forms a negative ion $(CF^-)^*$. Using the same approximation ,the $^3\Sigma^-$ and $^1\Delta$ resonances form vibrationally excited negative ions $(CF^-)^*$ which do not dissociate. It is likely that states of $(CF^-)^*$ resonances which do not lead to DEA will auto-ionise leading to vibrational excitation of the target. The widths of resonances were not taken into account in the above estimates. The dissociative electron attachment (DEA) cross section can be estimated as 50%

of the cross section for the excitation of the $^1\Sigma^+$ resonance (Fig. 11, Table VI). This estimate is very crude and gives an error value of about 50%. Following this assumption, the DEA cross section for CF has a peak at 1.76 x 10^{-20} m^2 for the electron energy of 2.19 eV. The DEA cross section data can be found in the electronic archive.

The threshold for dissociation into neutrals for the A $^2\Sigma^+$ state of CF is estimated to be 5.87 eV (v = 5). All vibrational states of A $^2\Sigma^+$ above v = 5 dissociate to C(^{3}P) + F(^{2}P); vibrational states below v = 5 may dissociate to the same limit. Our calculations also show that all vibrational states of the B $^2\Delta$ state dissociate to C(^{3}P) + F(^{2}P). The dissociation of both states occurs *via* an avoided crossing.

In conclusion, the recent refined theoretical calculations on electron interactions with CF has led to a deeper understanding of its dissociation properties and role in fluorocarbon plasmas. Similar studies have been performed for the related radicals CF_2 ans CF_3 and these will now be discussed.

5. CF_2

The ionization cross section for the CF_2 radical has been reported by Tarnovsky and Becker [21] and by Tarnovsky *et al* [22] in the energy range 10 - 200 eV. Later Deutsch *et al* [42] calculated the electron impact ionization cross section for CF_2 using the semiclassical Deutsch-Märk formalism and found that their cross section lies significantly above the measured data. Recently Joshipura *et al* [35] calculated the electron impact ionization cross section for the CF_2 radical in the energy range 20 - 2000 eV using the complex scattering potential approach. Their cross section is also higher (by about 50%) than the experimental one. This disagreement between experimental and theoretical results is certainly due to the crude models used in the calculations. No experimental data on low energy (below 10 eV) electron collisional cross sections for the CF_2 radical have been reported in the literature.

Figure 12A displays the total integral elastic and excitation cross sections for CF_2 at its equilibrium geometry and energies below 10 eV obtained using the UK-molecular R-matrix method [45]. Details of these calculations can be found in Rozum *et al* [16]. The electron impact excitation cross sections are divided into three groups: the cross section for the excitation of the metastable $^3B_1$ state (Fig. 12B), the cross section for the excitation of the bound and radiative $^1B_1$ state (Fig. 12C) and the sum of cross sections for the excitation of the remaining dissociative $^3A_2$, $^1A_2$ and $^3B_2$ states (Fig. 12D). The corresponding data are presented in Table VII.

The main feature in the elastic cross section (Fig. 12A) is the presence of a shape resonance of the $^2B_1$ symmetry. At equilibrium geometry this resonance has position and width of 0.95 eV and 0.18 eV respectively. This is a shape resonance which binds an extra electron in $3b_1$ orbital. Performing calculations, where one C-F bond was stretched from 1.8 to 3.6 a_0 with the other C-F bond and a CFC angle frozen, we found that the $^2B_1$ resonance becomes bound for C-F bond lengths greater than 3.2 a_0. The reflection approximation suggests that approximately 5% of the $^2B_1$ resonance asymptotically may dissociate to CF($^2\Pi$) + F^-(^{1}S) and 95% of the resonance forms a vibrationally excited negative ion $(CF_2^-)^*$. The DEA cross section for CF_2, estimated as 50% of the cross section for the excitation of the $^2B_1$ resonance, peaks at 25.76 x 10^{-20} m^2 for the incident electron energy of 0.95 eV. As was mentioned earlier, this assumption is crude and gives an error about 50%. The DEA cross section itself is shown in Fig. 13 and the cross section data can be found in Table VII.

The excitation process $^1A_1 \longrightarrow {}^3B_1$ (Fig. 12B) is dominated by the $^2A_1$ shape resonance with a position and width of 5.61 eV and 2.87 eV respectively at equilibrium. This resonance is very broad and short lived and could not be detected at a C-F bond length beyond 2.7 a_0.

Figure 14 and Table VII display the MTCS cross section and its data in the scattering energy range 0.1 – 10 eV. This cross section was obtained using the *POLYDCS* program and K-matrices generated during R-matrix calculations. The cross section contains several resonant structures. The lowest in energy structure corresponds to the $^2B_1$ resonance also present in the elastic cross section.

Our calculations suggest that all vibrational states of the $^3A_2$, $^1A_2$ and $^3B_2$ states of CF dissociate to CF($^2\Pi$) + F(^{2}P).

6. CF_3

The absolute partial electron-impact ionization cross section for CF_3 was measured by Tarnovsky and Becker [21] and may be compared with the recent calculations of Joshipura *et al* [32]. The agreement is once again good at high energies but the theory may be less reliable at energies below 100 eV. Diniz *et al* [49] calculated the elastic differential cross sections for electron collision with CF_3 in the energy range below 30 eV using the Schwinger multichannel method at the static-exchange level. They found that the elastic differential cross section for electron scattering from CF_3 was very similar to that from CF_3H reflecting that the role of the H atom in the scattering is small. Furthermore, the similarity between the two differential cross sections improves as the incident energy of the electron increases and the effect of the local charge cloud/molecular structure is reduced. Differential cross sections obtained by Rozum *et al* [19] agree reasonably with Diniz *et al's* results, but are about 40% higher in the forward direction. No experimental data on low-energy (sub 10 eV) collisional integral cross sections for the CF_3 radical have been reported.

Integral cross sections for low-energy electron scattering by the CF_3 radical have been calculated using the R-matrix method and a target model which gives satisfactory target parameters. Details of the target and scattering calculations have been given in Rozum *et al* [18] and will not be repeated here. The elastic cross section and electron impact excitation cross sections for the excitation to the A $^2A_2$, B ^2E and 2 ^2E are presented in Fig. 15. The corresponding cross section data are given in Table VIII. All the cross sections are presented here at the equilibrium geometry of CF_3.

Present calculations show the absence of any low-lying resonances which means that CF_3 will not undergo dissociative electron attachment (DEA). All our calculations show the presence of a bound state of the $^1A_1$ symmetry with a vertical binding energy estimated from pure bound state calculations to be 0.6 eV.

The momentum transfer cross section for electron scattering by CF_3 are shown in Fig. 16. Table VIII presents the MTCS data for CF_3. It can be seen that the momentum transfer cross section does not have any resonance-like features, again in contrast to those of CF and CF_2.

7. CONCLUSIONS

In this paper we present new and summarize existing recommended data on the electron collision cross sections with the radicals CF, CF_2 and CF_3, and the etching gases CF_3I and C_2F_4. Numerical values are tabulated in the paper and can also be found in the electronic archive.

Elastic and excitation integral and momentum transfer cross sections for the CF_x radicals are calculated in the energy range 100 meV – 10 eV and presented in a form relevant to the modelling of etching plasmas. Thus, electron impact excitation cross sections were divided into three main groups: i) excitation of metastable states, ii) excitation of dissociative states, iii) excitation of other states. Even though there is no experimental data on the integral cross sections for the CF_x radicals available, we regard our results as reliable for energies above 100 meV. This confidence is in part due to the fact that our previous low-energy electron collision calculations for the OClO radical of Baluja *et al* [50] gave generally excellent agreement with experimental measurements in the 0.1 eV to 10 eV energy range.

Our calculations show that CF and CF_2 support rich low-energy resonant structures. It is well known that some low-energy resonances provide routes to dissociative electron attachment. The fate of these resonances is estimated using the reflection approximation. The resonance widths are not taken into account in the present work, therefore, these estimates are not precise. Dissociative attachment cross sections for CF_x are estimated as 50% of the cross sections for the excitation of individual resonances. This estimate is crude and has an error of about 50%.

The ($CF + e^-$) system has three low-energy shape resonances in the integral elastic cross section, which are $^3\Sigma^-$, $^1\Delta$ and $^1\Sigma^+$. These resonances become bound at C-F bond lengths larger than 2.5 a_0 ($^3\Sigma^-$), 3.3 a_0 ($^1\Delta$) and 3.6 a_0 ($^1\Sigma^+$). The reflection approximation suggests that about 20% of the $^1\Sigma^+$ resonance may asymptotically dissociate to $C(^1D) + F^-(^1S)$ and the remaining 80% forms a negative ion $(CF^-)^*$, while the $^3\Sigma^-$ and $^1\Delta$ resonances form vibrationally excited negative ions $(CF^-)^*$. It is likely that states of $(CF^-)^*$ resonances which do not lead to DEA will auto-ionise leading to vibrational excitation of the target. We estimate the DEA cross section of CF which peaks at 1.76 x 10^{-20} m^2 for the incident electron energy of 2.19 eV.

The $^2B_1$ resonance in the integral elastic cross section of CF_2 is assigned. This resonance becomes bound at C-F bond lengths greater than 3.2 a_0. From the reflection approximation about 5% of the $^2B_1$ resonance asymptotically may dissociate to $CF(^2\Pi) + F^-(^1S)$ and 95% of the resonance forms a vibrationally excited negative ion $(CF_2^-)^*$. The DEA cross section for CF_2 is estimated to peak at 25.76 x 10^{-20} m^2 for the electron energy of 0.91 eV.

Like the integral elastic and excitation cross sections, momentum transfer cross sections for CF and CF_2 presented here have several low energy resonant structures. Some of these structures correspond to resonances also present in the integral elastic cross sections.

In contrast to calculations on CF and CF_2, our calculations on CF_3 show the absence of any low-lying resonances. The integral elastic cross section and the momentum transfer cross section for CF_3 therefore do not have any resonant structures. The absence of any low-lying resonances in the ($CF_3 + e^-$) system means that CF_3 will not undergo DEA under standard etching plasma conditions. This may have significant implications for plasma processing. Firstly, the low anion density in a plasma formed from a CF_3 precursor feed gas may lead to a significant reduction of the sheath above the sample. This will change the cation energies and transport properties to the surface [51, 52]. Secondly, anions act as nuclei for polymerization reactions [53], which form the so-called 'dust'. This 'dust' has to be periodically removed from the reactor thus leading to a costly down time in the processing plant. Furthermore, it has been estimated that between 60% and 90% of the current perfluorocarbon emissions of industrial plasma reactors take place during the cleaning of the chambers [54]. Consequently, the feed gas based on CF_3I rather then C_2F_4 could significantly affect the formation of polymers in the reactor and the ion etching rate.

8. ACKNOWLEDGEMENTS

We thank Prof. Jean-Paul Booth for many helpful discussions and encouraging to write this paper. We also acknowledge the data provided on the integral and momentum transfer cross sections by Prof. Marco Lima,

electron ionization cross sections by Prof. Tilmann Märk, and Dr. Garscadden. Prof. Vincent McKoy and Prof. Carl Winstead are also acknowledged for the data provided in this paper on the integral elastic and momentum transfer cross sections. Prof. Joshipura and Dr. B. Antony are also acknowledge for the provided data.

PLV acknowledges the honorary researcher fellow position at University College London during the preparation of this manuscript, SE and NJM acknowledge the support of UK funding councils EPSRC, NERC and CLRC. IR would like to thank the British Government and EPSRC, JT acknowledges EPSRC for financial support.

Most of the calculations on CF_x radicals were performed on Sunfire computer Ra at the UCL Hiperspace computer centre.

[1] B. Graham, Physics World **14**, 31 (2001).
[2] M. A. Lieberman and A. J. Lichtenberg, Principles of Plasma Discharges and Material Processing, Wiley, New York (1994).
[3] A. 1997 (1997).
[4] T. Goto, Adv. At. Mol. Phys. **44**, 99 (2001).
[5] T. Makabe, Adv. At. Mol. Phys. **44**, 127 (2001).
[6] S. Raoux, M. B. T. Tanaka, H. Ponnekanti, M. Seamons, T. Deacon, L. Xia, F. Pham, D. Silvetti, D. Cheung, and K. Fairbairn, J. Vac. Sci. Technol. B **71(2)**, 477 (1999).
[7] IPCC, International Panel on Climate Change, The Third Assessment Report, www.ipcc.ch (2001).
[8] S. Solomon, J. B. Burkholder, A. R. Ravishankara, and R. R. Garcia, J. Geophysical Research **99**, 20929 (1994).
[9] G. Acerboni, J. A. Buekes, N. R. Jensen, J. Hjorth, G. Myhre, C. J. Nielsen, and J. K. Sundet, Atm. Environ. **35**, 4113 (2001).
[10] S. Samukawa and T. Mukai, J. Vac. Sci. Technol. A **17**, 2551 (1999).
[11] T. Oster, O. Ingólfsson, M. Meinke, T. Jaffke, and E. Illenberger, J. Chem. Phys. **99**, 5141 (1993).
[12] T. K. Minton, P. Felder, R. C. Scales, and J. R. Huber, Chem. Phys. Lett. **164**, 113 (1989).
[13] S. Samukawa, T. Mukai, and K. Noguchi, Mater. Sci. Semicond. Process. **2**, 203 (1999).
[14] L. G. Christophorou and J. K. Olthoff, J. Phys. Chem. Ref. Data **29(4)**, 553 (2000).
[15] L. G. Christophorou and J. K. Olthoff, Appl. Surf. Sci. **192**, 309 (2002).
[16] I. Rozum, N. J. Mason, and J. Tennyson, J. Phys. B: At. Mol. Opt. Phys. **35**, 1583 (2002).
[17] I. Rozum, N. J. Mason, and J. Tennyson, J. Phys. B: At. Mol. Opt. Phys. **36**, 2419 (2003a).
[18] I. Rozum, N. J. Mason, and J. Tennyson, New J. Phys. **5**, 155.1 (2003b).
[19] I. Rozum and J. Tennyson, J. Phys. B: At. Mol. Opt. Phys. **37**, 957 (2004).
[20] L. G. Christophorou, Plenary Talks, The Technological Plasmas Workshop, Birmingham, UK (2003).
[21] V. Tarnovsky and K. Becker, J. Chem. Phys. **98**, 7868 (1993).
[22] V. Tarnovsky, P. Kurunczi, D. Rogozhnikov, and K. Becker, Int. J. Mass Spectrom. Ion Processes **128**, 181 (1993).
[23] M. H. Bettega, A. Natalense, M. Lima, and L. G. Ferreira, J. Phys. B: At. Mol. Opt. Phys. **34**, 4041 (2003).
[24] N. J. Mason, P. L. ao Vieira, S. Eden, P. Kendall, S. Pathak, A. Dawes, J. Tennyson, P. Tegeder, M. Kitajima, M. Okamoto, et al., Intern. J. Mass Spectrom. **223**, 647 (2003).
[25] C. Szmytkowski, S. Kwitnewski, and E. Ptasiska-Denga, Phys. Rev. A **68**, 032715 (2003).
[26] C. Winstead and V. McKoy, J. Chem. Phys. **116**, 1380 (2002).
[27] S. Eden, P. Limão-Vieira, P. A. Kendall, N. J. Mason, J. Delwiche, M. Hubin-Franskin, T. Tanaka, M. Kitajima, H. Tanaka, H. Cho, et al., Chem. Phys. **297**, 257 (2004).
[28] M. Kitajima, M. Okamoto, K. Sunohara, H. Tanaka, H. Cho, S. Samukawa, S. Eden, and N. J. Mason, J. Phys. B: At. Mol. Opt. Phys. **35**, 3257 (2002).
[29] K. Sunohara, M. Kitajima, H. Tanaka, M. Kimura, and H. Cho, J. Phys. B: At. Mol. Opt. Phys. **36**, 1843 (2003).
[30] M. Kitajima, R. Suzuki, H. Tanaka, L. Pichl, and H. Cho, Nukleonika **48**, 89 (2003).
[31] M. K. Kawada, O. Sueoka, and M. Kimura, Chem. Phys. Lett. **330**, 34 (2000).
[32] K. N. Joshipura, V. Minaxi, C. G. Limbachiya, and B. K. Antony, Phys. Rev. A **in press** (2004).
[33] C. Q. Jiao, G. Ganguly, C. A. DeJoseph, and A. Garscadden, Int. J. Mass Spectrom. **208**, 127 (2001).
[34] U. Onthong, H. Deutsch, K. Becker, S. Matt, M. Probst, and T. D. Märk, Int. J. Mass Spectrom. **214**, 53 (2002).
[35] K. N. Joshipura, M. Vinodkumar, B. K. Antony, and N. J. Mason, Eur. Phys J. D **23**, 81 (2003).
[36] T. Nakumura, H. Motomura, and K. Tachibana, Jpn. J. Appl. Phys. **30**, 847 (2001).
[37] Y. Jiang, J. Sun, and L. Wan, Phys. Rev. A **62**, 062712 (2000).
[38] K. Yoshida, S. Goto, H. Tagashira, C. Winstead, B. V. McKoy, and W. L. Morgan, J. Appl. Phys. **91**, 2637 (2002).
[39] E. Illenberger, H. Baumgärtel, and S. Süzer, J. Electron. Spectrosc. Relat. Phenom. **33**, 123 (1984).
[40] A. N. Goyette, J. de Urquijo, Y. Wang, L. G. Christophorou, and J. K. Olthoff, J. Chem. Phys. **114**, 8932 (2001).
[41] M. Bobeldijk, W. Zande, and P. J. Kistemaker, Chem. Phys. **179**, 125 (1994).
[42] H. Deutsch, K. Becker, S. Matt, and T. D. Märk, Int. J. Mass Spectrom. **197**, 37 (2000).
[43] W. M. Huo, V. Tarnovsky, and K. H. Becker, Chem. Phys. Lett. **358**, 328 (2002).
[44] M. T. Lee, L. M. Brescansin, L. E. Machado, and F. Machado, Phys. Rev. A **66**, 012720 (2002).
[45] L. A. Morgan, J. Tennyson, and C. J. Gillan, Comput. Phys. Commun. **114**, 120 (1998).
[46] N. Sanna and F. A. Gianturco, Comput. Phys. Commun. **114**, 142 (1998).
[47] T. L. Porter, D. E. Mann, and N. Acquista, J. Mol. Spectrosc. **16**, 228 (1965).
[48] B. S. Jursic, Theor. Chem. Acc. **99**, 289 (1998).

[49] R. B. Diniz, M. Lima, and F. J. Paixão, J. Phys. B: At. Opt. Mol. Phys. **32**, L539 (1999).
[50] K. L. Baluja, N. J. Mason, L. A. Morgan, and J. Tennyson, J. Phys. B: At. Opt. Mol. Phys. **34**, 4041 (2001).
[51] R. N. Franklin and J. Snell, J. Phys. D: Appl. Phys. **33**, 1990 (2000).
[52] R. N. Franklin, J. Phys. D: Appl. Phys. **35**, 536 (2002).
[53] E. Stoffels, W. W. Stoffels, and K. Tachibana, J. Vac. Sci. Technol. A **16**, 87 (1998).
[54] L. Beu and P. T. Brown, Semiconductor Fabtech **11**th **edition**, 91 (2000).

TABLE II: Electronic archive tables.

Table	Description
Table 1	Data on the total electron scattering cross section for CF_3I.
Table 2	Data on the momentum transfer cross section for CF_3I.
Table 3	Data on the integral elastic scattering cross section for CF_3I.
Table 4	Data on the ionization cross section for CF_3I.
Table 5	Data on the electron attachment cross section for CF_3I.
Table 6	Data on the integral elastic electron scattering cross section for C_2F_4.
Table 7	Data on the momentum transfer cross section for C_2F_4.
Table 8	Data on the ionization cross section for C_2F_4.
Table 9	Data on the momentum transfer cross section for CF.
Table 10	Data on the total elastic cross section, electron impact excitation cross sections for the excitation of the metastable a $^4\Sigma^-$ state, dissociative A $^2\Sigma^+$ and B $^2\Delta$ states, and other states C $^2\Sigma^-$ and b $^4\Pi$ for CF.
Table 11	Estimated data on the dissociative electron attachment cross section for CF.
Table 12	Data on the total integral elastic, electron impact excitation cross sections for the excitation of the metastable $^3B_1$ state, bound and radiative $^1B_1$ state, and remaining dissociative $^3A_2$, $^1A_2$ and $^3B_2$ states for CF_2.
Table 13	Estimated data on the dissociative electron attachment cross section for CF_2.
Table 14	Data on the momentum transfer cross section for CF_2.
Table 15	Data on the elastic cross section and electron impact excitation cross sections for the excitation of the A $^2A_2$, B ^2E and 2 ^2E states for CF_3.
Table 16	Data on the momentum transfer cross section for CF_3.

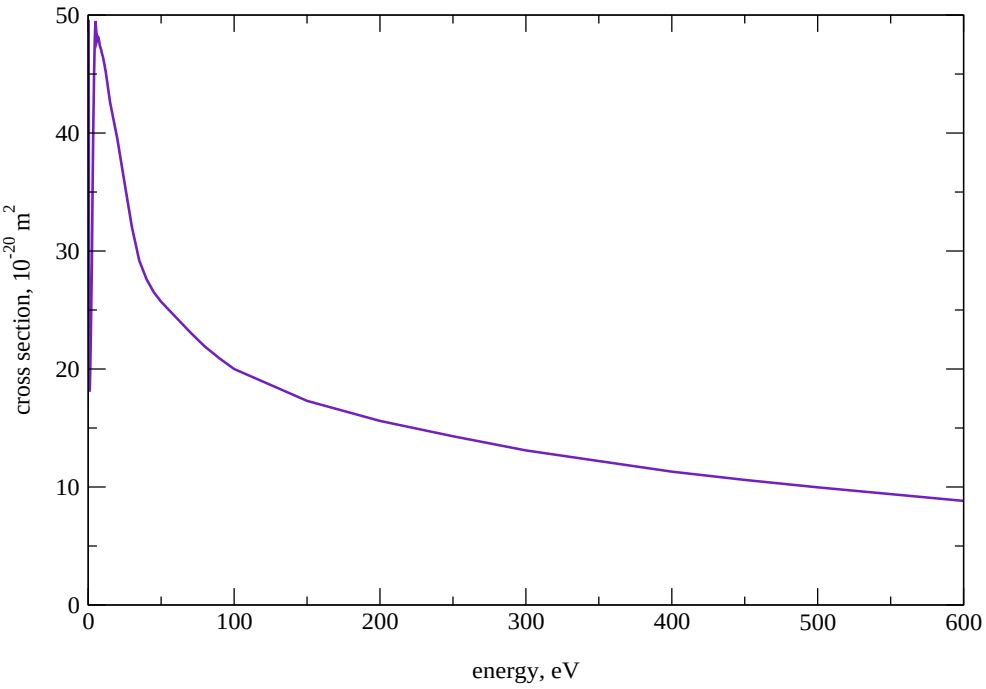

FIG. 1: Total electron scattering cross section for CF_3I (Christophorou and Olthoff 2000).

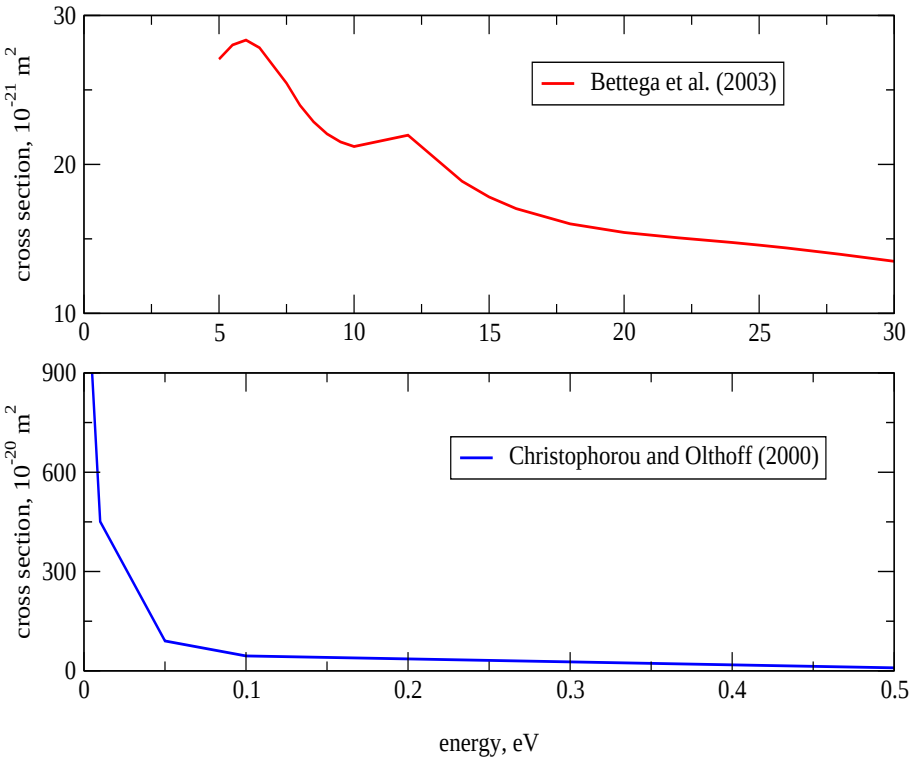

FIG. 2: Momentum transfer cross sections for CF_3I.

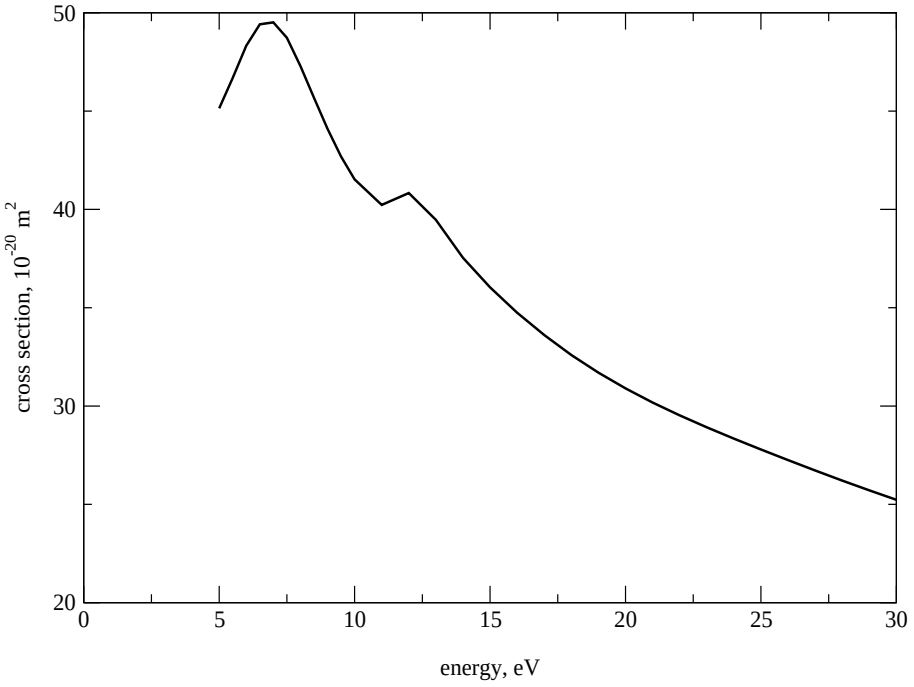

FIG. 3: Integral elastic cross section for CF_3I (Bettega *et al* 2003).

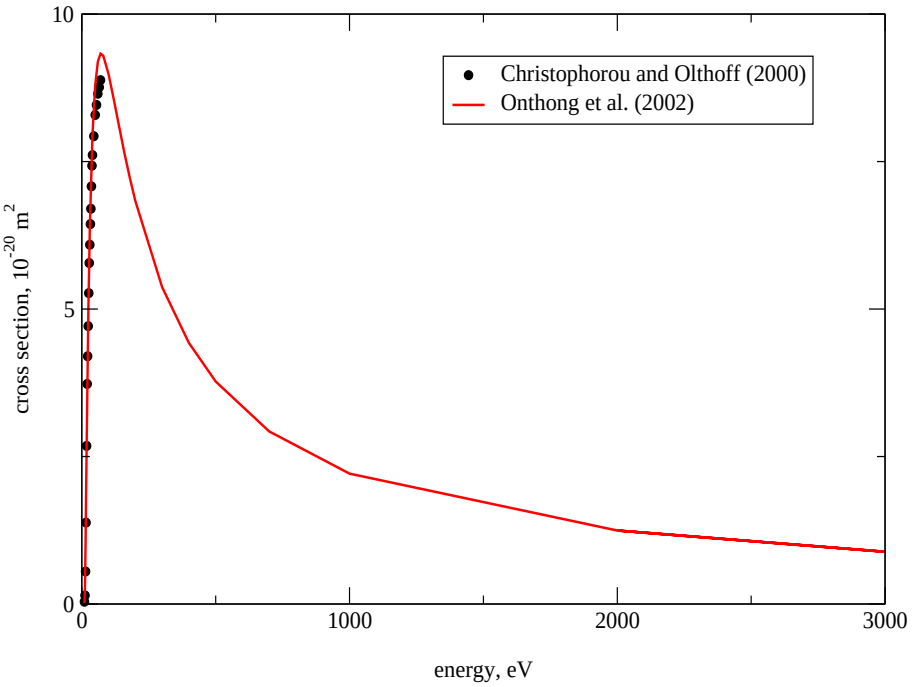

FIG. 4: Ionization cross sections for CF_3I.

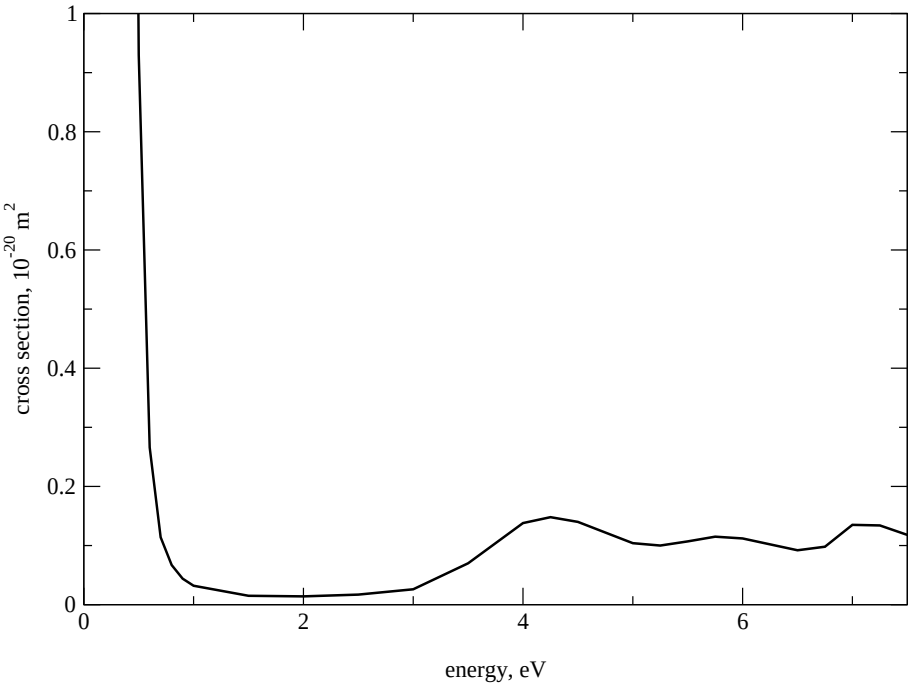

FIG. 5: Electron attachment cross section for CF_3I (Christophorou and Olthoff 2000).

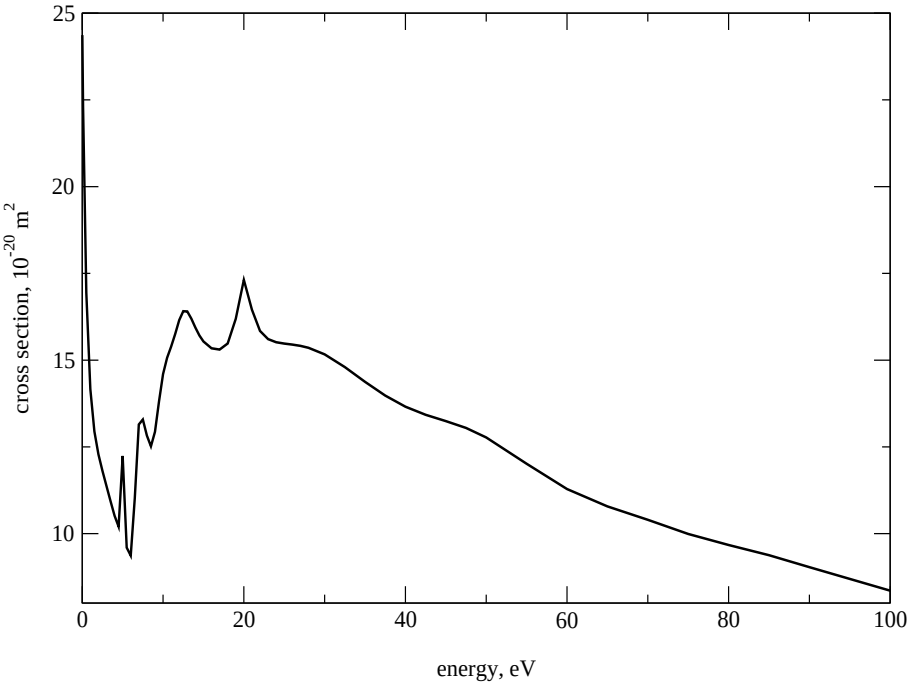

FIG. 6: Momentum transfer cross section for C_2F_4 (Winstead and McKoy 2002).

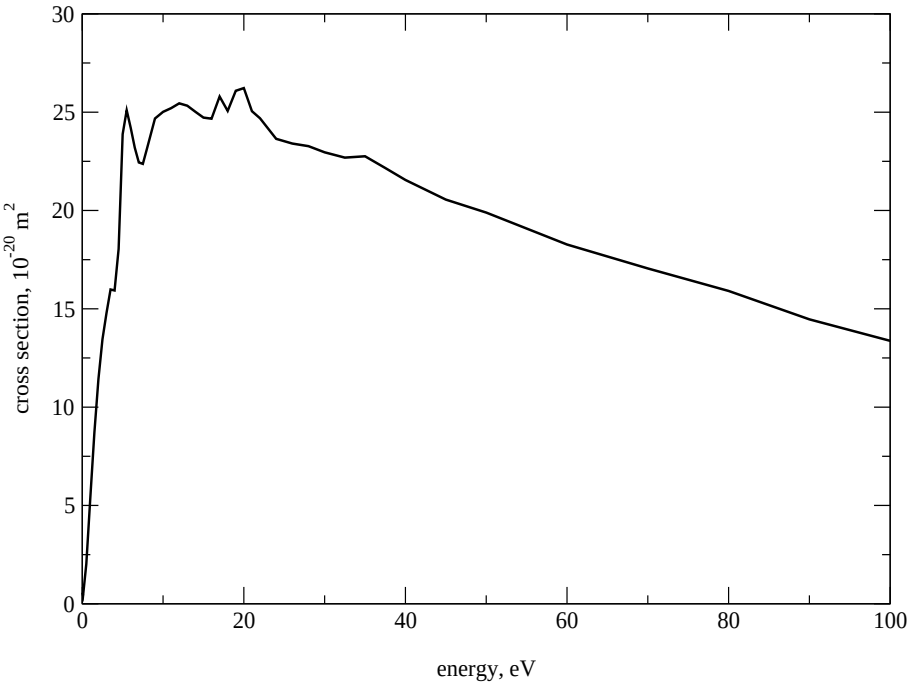

FIG. 7: Integral elastic electron scattering cross section for C_2F_4 (Winstead and McKoy 2002).

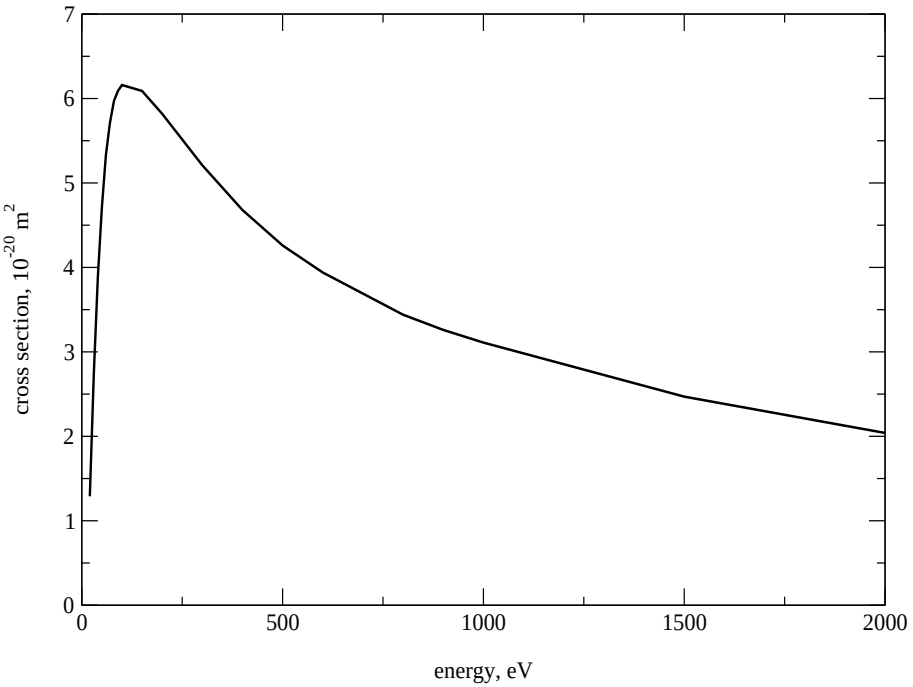

FIG. 8: Electron impact ionization cross section for C_2F_4 (Joshipura *et al* 2004).

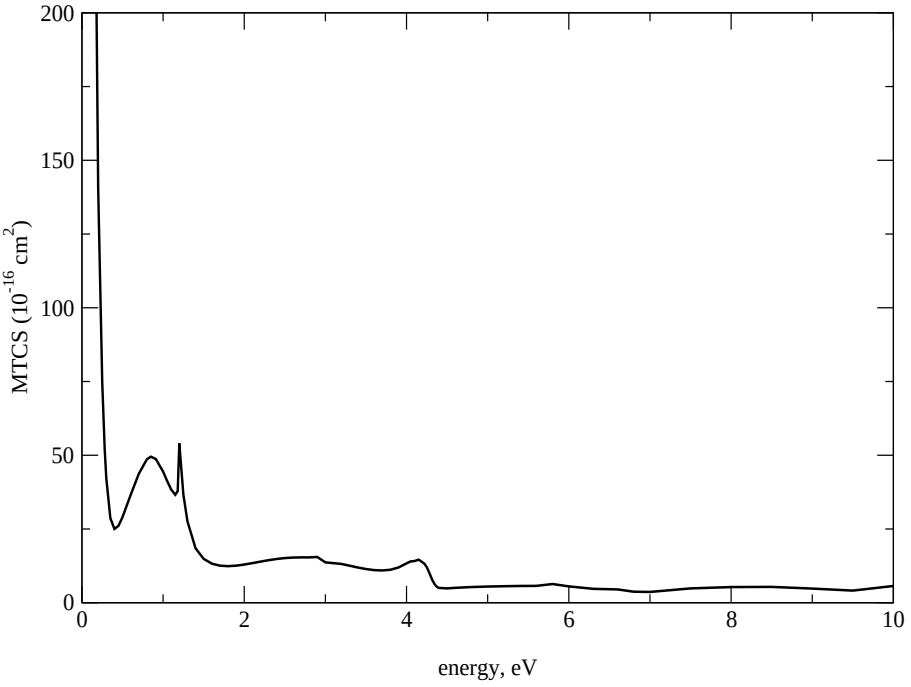

FIG. 9: Momentum transfer cross section for electron scattering by CF.

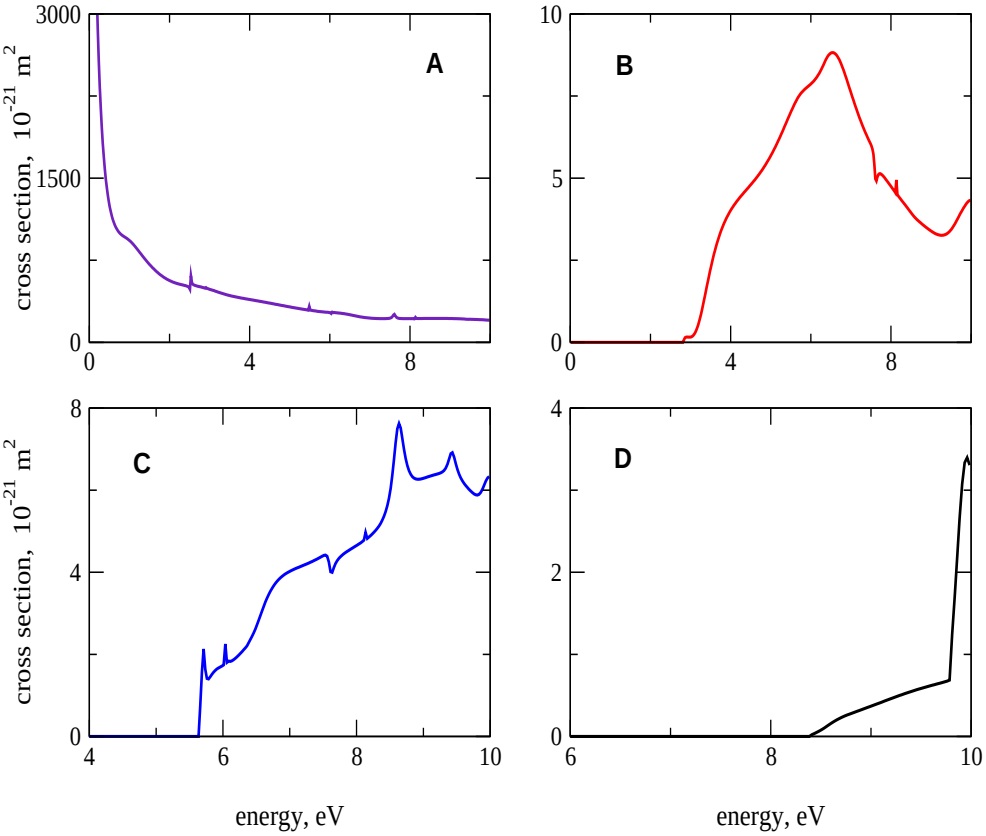

FIG. 10: Total elastic cross sections for electron scattering off CF (A); electron impact excitation cross sections for the excitation of the metastable a $^4\Sigma^-$ state (B), dissociative A $^2\Sigma^+$ and B $^2\Delta$ states (C) and other states C $^2\Sigma^-$ and b $^4\Pi$ (D).

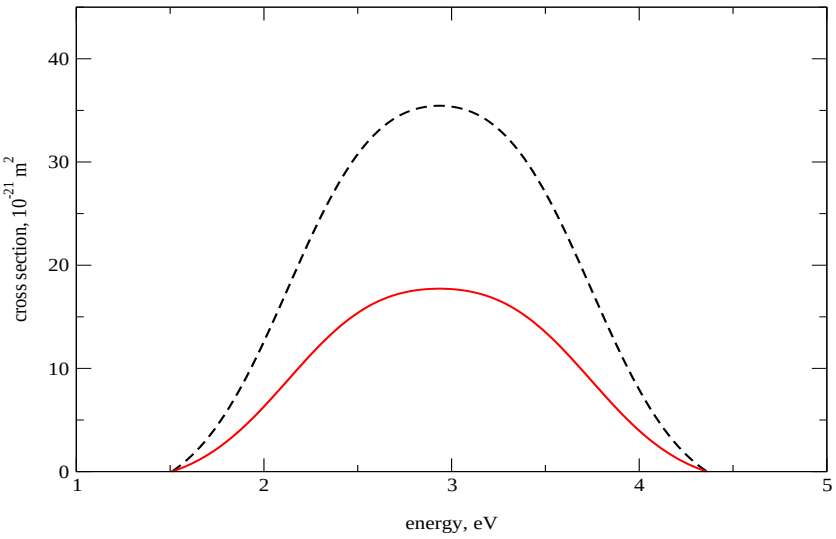

FIG. 11: Dissociative electron attachment cross section for CF (solid line) estimated as 50% of the cross section for the excitation of the $^1\Sigma^+$ resonance (dashed line).

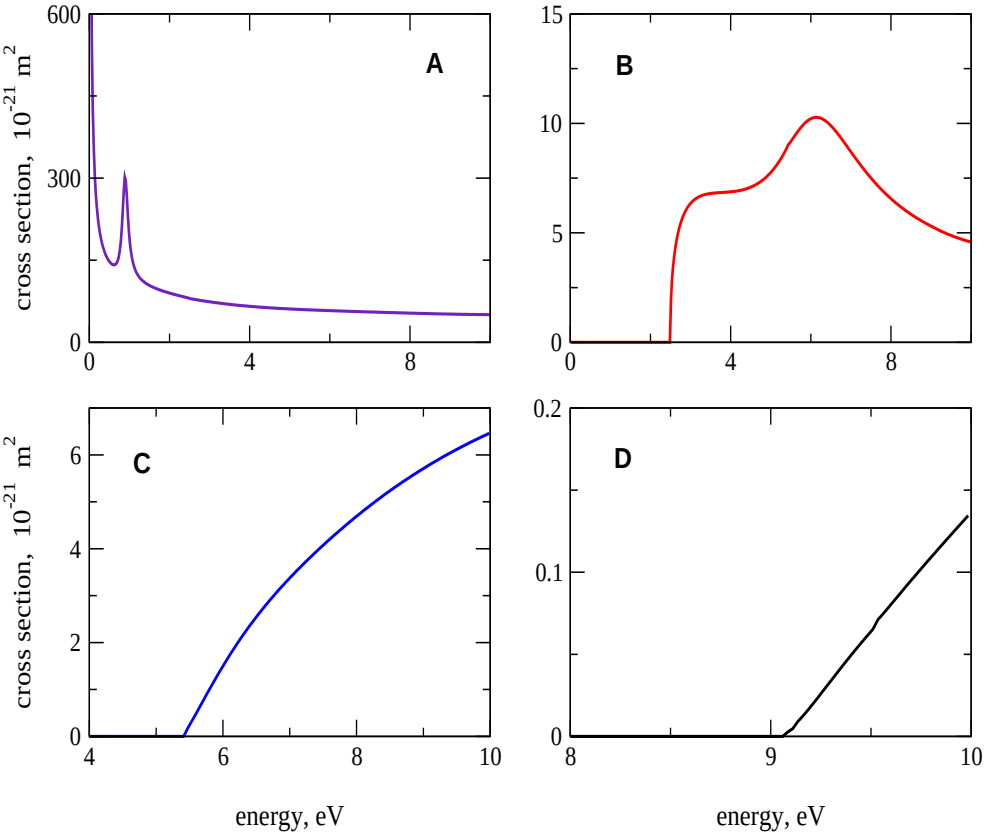

FIG. 12: Total elastic cross sections for electron scattering off CF_2 (A); electron impact excitation cross sections for the excitation of the metastable $^3B_1$ state (B), bound and radiative $^1B_1$ state (C) and other dissociative $^3A_2$, $^1A_2$ and $^3B_2$ states (D).

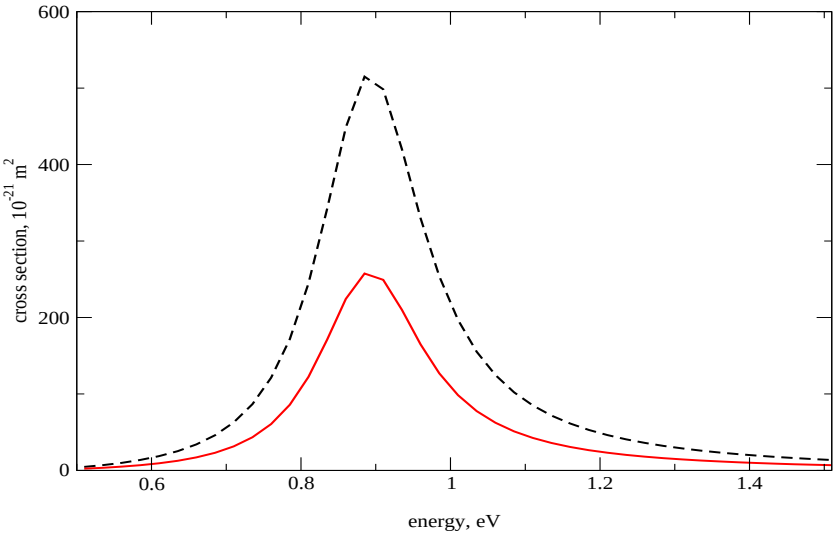

FIG. 13: Dissociative electron attachment cross section for the CF_2 radical (solid line) estimated as 50% of the cross section for the excitation of the $^2B_1$ resonance (dashed line).

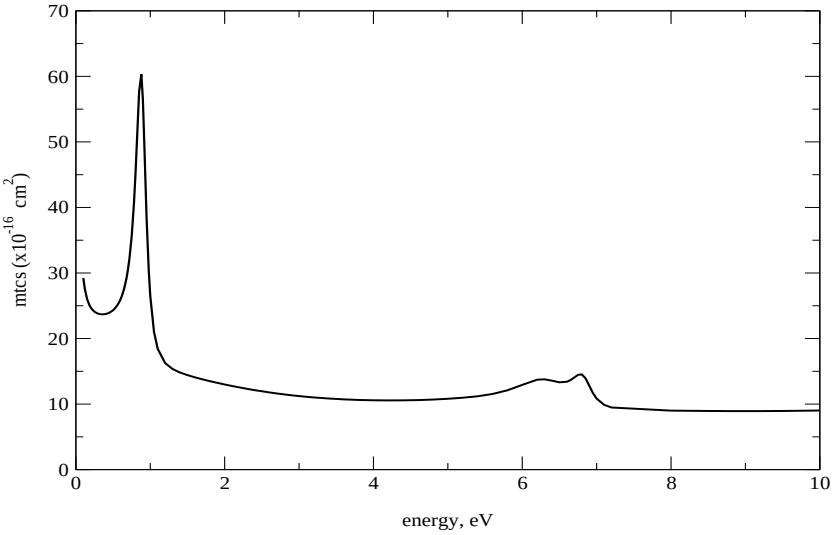

FIG. 14: Momentum transfer cross section for electron collisions with the CF_2 radical.

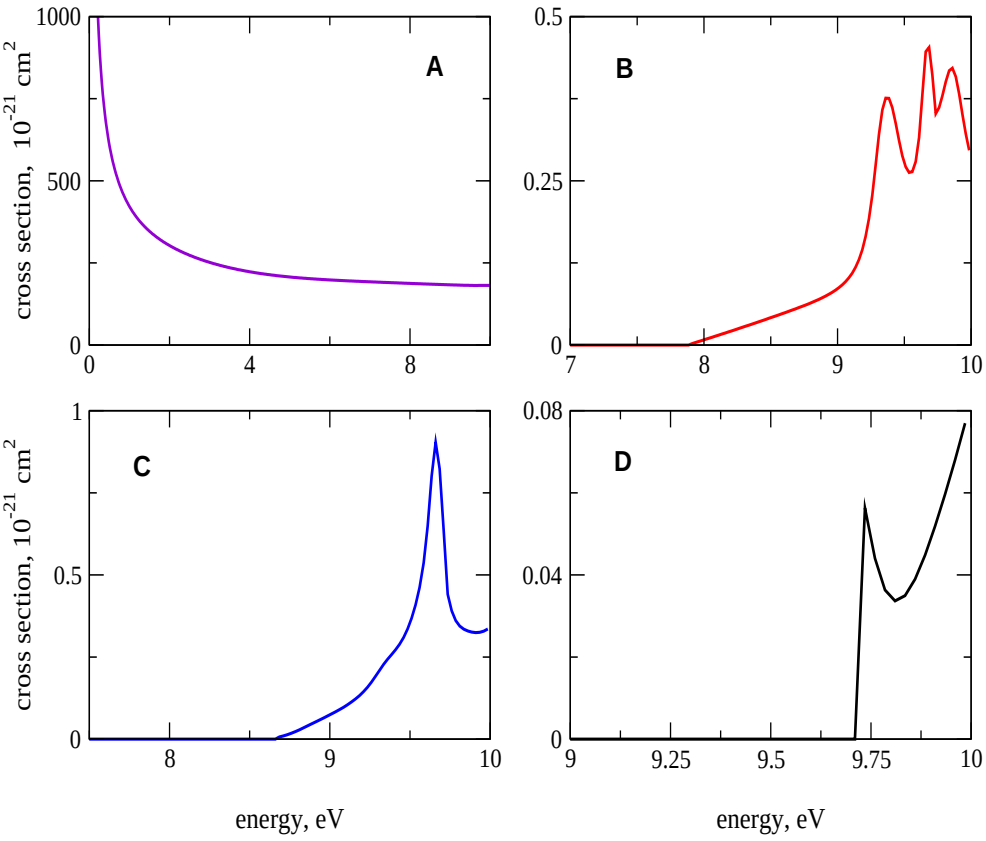

FIG. 15: Total elastic cross sections for electron scattering off CF_3 (A); electron impact excitation cross sections for the excitation of the first excited A $^2A_2$ state (B), second excited B ^2E state (C) and third excited 2 ^2E state (D).

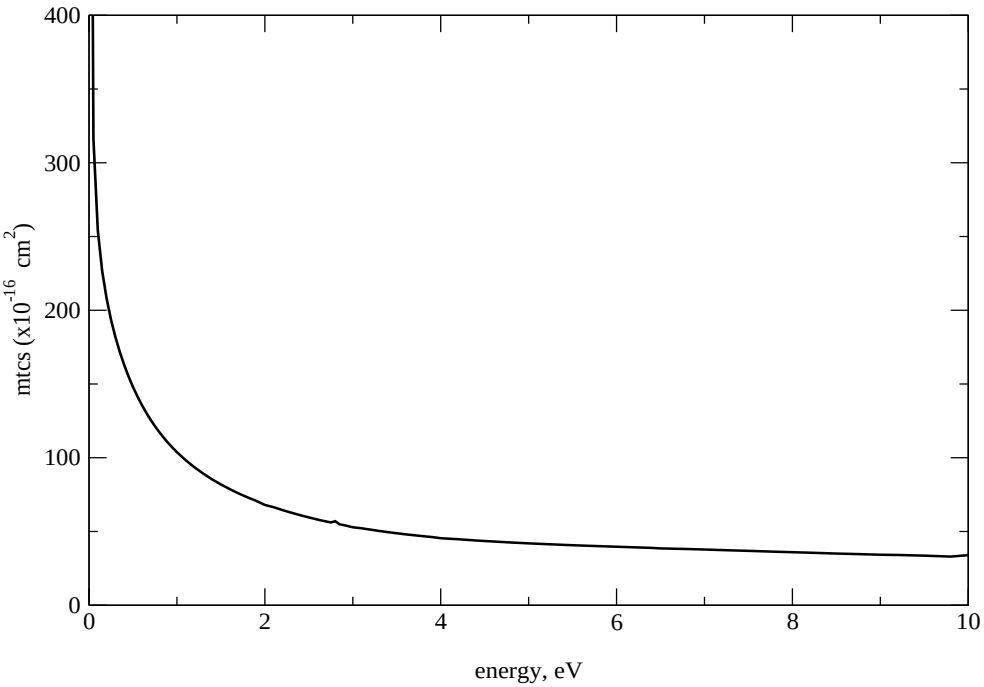

FIG. 16: Momentum transfer cross section for electron scattering by the CF_3 radical.

TABLE III: Data on the electron scattering cross sections for CF_3I. Energies (E) are given in eV; cross sections are given in 10^{-20} m^2. Key:
TXT - total electron scattering cross section;
MTXC - momentum transfer cross section.

E	TXT[a]	E	MTXT[b]	E	MTXT[a]
0.3	49.6	5	27.06271231	0.005	902
0.4	40.5	5.5	28.02126848	0.01	451
0.5	31.5	6	28.34768062	0.05	90.2
0.6	23.3	6.5	27.8302742	0.1	45.1
0.7	19.8	7	26.63651167	0.5	9
0.8	18.8	7.5	25.45486906		
0.9	18.2	8	23.96789193		
1	18.1	8.5	22.86108719		
1.25	19.1	9	22.04912014		
1.5	20.7	9.5	21.50976299		
1.75	22.4	10	21.19957323		
2	24.3	12	21.96245058		
2.5	29	14	18.86652762		
3	35.3	15	17.81201957		
3.5	40.5	16	17.03199636		
4	44.9	18	16.00920269		
4.5	47.9	20	15.43238323		
5	49.5	22	15.06993597		
5.5	48.6	24	14.75454956		
6	47.9	25	14.58181211		
6.5	48.2	26	14.39162657		
7	48.1	28	13.96217417		
7.5	47.8	30	13.49639282		
8	47.4	28	13.96217417		
8.5	47.2	30	13.49639282		
9	47				
9.5	46.7				
10	46.5				
11	45.9				
12	45.2				
15	42.6				
20	39.5				
25	35.7				
30	32				
35	29.2				
40	27.6				
45	26.5				
50	25.7				
60	24.4				
70	23.1				
80	21.9				
90	20.9				
100	20				
150	17.3				
200	15.6				
250	14.3				
300	13.1				
350	12.2				
400	11.3				
450	10.6				
500	9.97				
600	8.82				

[a] From Cristophorou and Olthoff (2000).
[b] From Bettega *et al* (2003).

TABLE IV: Data on the electron scattering cross sections for CF_3I. Energies (E) are given in eV; cross sections are given in 10^{-20} m^2. Key:
IEXS - integral elastic electron scattering cross section;
IONXS - electron impact ionization cross section;
TEAXS - total electron attachment cross section.

E	IEXS[a]	E	IONXS[b]	E	IONXS[c]	E	TEAXS[d]
5	45.13802309	10	0.039	10	0.000225	0.004	1820
5.5	46.68473228	12	0.146	12	0.316	0.005	1575
6	48.32475445	14	0.551	14	1.022	0.006	1399
6.5	49.41352903	16	1.38	16	1.83	0.007	1265
7	49.51293135	18	2.68	18	2.633	0.008	1157
7.5	48.72703988	20	3.73	20	3.398	0.009	1070
8	47.28897056	22	4.2	25	5.101	0.01	997
8.5	45.6807915	24	4.71	30	6.387	0.015	757
9	44.09751828	26	5.27	40	7.953	0.02	623
9.5	42.68394624	28	5.78	50	8.796	0.025	532
10	41.52693803	30	6.09	60	9.194	0.03	464
11	40.22742639	32	6.44	70	9.328	0.04	369
12	40.83230831	34	6.7	80	9.296	0.05	302
13	39.47192285	36	7.08	100	8.983	0.06	251
14	37.53890715	38	7.43	120	8.542	0.07	212
15	36.0355929	40	7.61	140	8.077	0.08	183
16	34.74823476	45	7.93	160	7.629	0.09	158
17	33.6096065	50	8.29	180	7.212	0.1	139
18	32.59754473	55	8.46	200	6.83	0.15	76.1
19	31.69822251	60	8.65	300	5.372	0.2	39.4
20	30.89753305	65	8.76	400	4.427	0.25	19.9
21	30.17927355	70	8.88	500	3.772	0.3	11.1
22	29.52581683			700	2.926	0.4	3.38
23	28.91962525			1000	2.21	0.5	0.93
24	28.34537193			2000	1.246	0.6	0.266
25	27.79167293			3000	0.885	0.7	0.114
26	27.25206673					0.8	0.067
27	26.72466439					0.9	0.044
28	26.21086512					1	0.032
29	25.71346453					1.5	0.015
30	25.2348021					2	0.014
29	25.71346453					2.5	0.017
30	25.2348021					3	0.026
						3.5	0.07
						4	0.138
						4.25	0.148
						4.5	0.14
						4.75	0.122
						5	0.104
						5.25	0.1
						5.5	0.107
						5.75	0.115
						6	0.112
						6.25	0.102
						6.5	0.092
						6.75	0.098
						7	0.135
						7.25	0.134
						7.5	0.118

[a] From Bettega *et al* (2003).
[b] From Cristophorou *et al* (2000).
[c] From Onthong *et al* (2002).
[d] From Cristophorou and Onthong (2000).

TABLE V: Data on the electron scattering cross sections for C_2F_4. Key:
IEXS - integral elastic electron scattering cross section;
IONXS - electron impact ionization cross section;
MTXS - momentum transfer cross section.
Energies (E) are given in eV; cross sections are given in 10^{-20} m^2.

E	IEXS[a]	E	IONXS[b]	E	MTXS[a]	E	MTXS[a]
0.01	0.5694	20	1.29	0.01	24.365	17	15.3047
0.1	0.42	30	2.75	0.1	22.3108	18	15.4809
0.5	2.0206	40	3.89	0.5	16.9476	19	16.1926
1	5.411	50	4.71	1	14.1637	20	17.3144
1.5	8.7011	60	5.33	1.5	12.9466	21	16.4545
2	11.4197	70	5.71	2	12.2876	22	15.8412
2.5	13.4491	80	5.97	2.5	11.8079	23	15.6072
3	14.787	90	6.09	3	11.3698	24	15.5162
3.5	15.9821	100	6.16	3.5	10.9357	25	15.4766
4	15.9341	150	6.09	4	10.5149	26	15.4486
4.5	18.0437	200	5.82	4.5	10.2039	27	15.4119
5	23.8787	300	5.21	5	12.2401	28	15.3555
5.5	25.0965	400	4.68	5.5	9.5991	30	15.1656
6	24.1962	500	4.26	6	9.3674	32.5	14.8002
6.5	23.1963	600	3.94	6.5	11.0178	35	14.3748
7	22.4434	700	3.69	7	13.145	37.5	13.9783
7.5	22.3709	800	3.44	7.5	13.2906	40	13.6596
8	23.1296	900	3.26	8	12.8248	42.5	13.4263
9	24.6789	1000	3.11	8.5	12.5179	45	13.2444
10	25.016	1500	2.47	9	12.9342	47.5	13.0465
11	25.2023	2000	2.04	9.5	13.8109	50	12.7727
12	25.4501			10	14.5988	55	12.0141
13	25.3296			10.5	15.068	60	11.2869
14	25.0215			11	15.3907	65	10.7851
15	24.7248			11.5	15.7531	70	10.4
16	24.6682			12	16.1516	75	9.992
17	25.7959			12.5	16.4111	80	9.6727
18	25.061			13	16.4023	85	9.3788
19	26.0854			13.5	16.1967	90	9.0335
20	26.2226			14	15.938	100	8.3559
21	25.0519			14.5	15.7103		
22	24.6879			15	15.5375		
24	23.645			16	15.3407		
26	23.4057						
28	23.2717						
30	22.9597						
32.5	22.6896						
35	22.7577						
37.5	22.1617						
40	21.5524						
45	20.5532						
50	19.8962						
60	18.2698						
70	17.0511						
80	15.9077						
90	14.4625						
100	13.3694						

[a] From Winstead and McKoy (2002). [b] From Joshipura *et al* (2004).

TABLE VI: Data on the electron scattering cross sections for CF for selected energy points. Energies (E) are given in eV; cross sections are given in 10^{-21} m^2. The electronic archive presents the same data for 400 energy points. Key:
IEXS - integral alstic scattering cross section; EXC1 - excitation to the first excited $^4\Sigma^-$ state;
EXSD - excitation to the dissociative A $^2\Sigma^+$ and B $^2\Delta$ states; EXSO - excitation to other states C $^2\Sigma^-$ and b $^4\Pi$;
MTXS - momentum transfer cross section; DEA - estimated dissociative attachment cross section.

E	IEXS	EXC1	EXSD	EXSO	E	MTXS	E	DEA	E	DEA
0.110	4685.5737	0.0000	0.0000	0.0000	0.03	8055.9601	1.53	0.1678	3.66	10.5511
0.210	2852.7898	0.0000	0.0000	0.0000	0.05	6854.7998	1.56	0.3406	3.68	10.0469
0.310	1965.0991	0.0000	0.0000	0.0000	0.07	5742.9700	1.59	0.5294	3.71	9.5375
0.410	1492.9552	0.0000	0.0000	0.0000	0.10	4324.6799	1.61	0.7350	3.73	9.0250
0.510	1236.1290	0.0000	0.0000	0.0000	0.20	1405.8299	1.63	0.9578	3.76	8.5120
0.610	1095.6062	0.0000	0.0000	0.0000	0.25	748.1040	1.66	1.1985	3.79	8.0005
0.710	1020.0728	0.0000	0.0000	0.0000	0.28	523.1380	1.68	1.4576	3.81	7.4930
0.810	980.5687	0.0000	0.0000	0.0000	0.30	422.4950	1.71	1.7355	3.84	6.9915
0.910	955.6342	0.0000	0.0000	0.0000	0.35	286.9330	1.74	2.0324	3.86	6.4981
1.010	927.6247	0.0000	0.0000	0.0000	0.40	250.2610	1.76	2.3486	3.88	6.0148
1.110	889.3623	0.0000	0.0000	0.0000	0.45	260.4310	1.78	2.6842	3.91	5.5433
1.210	843.9416	0.0000	0.0000	0.0000	0.50	290.2420	1.81	3.0389	3.93	5.0853
1.310	796.6284	0.0000	0.0000	0.0000	0.60	365.1220	1.84	3.4126	3.96	4.6421
1.410	750.8224	0.0000	0.0000	0.0000	0.70	436.6470	1.86	3.8048	3.98	4.2149
1.510	708.2379	0.0000	0.0000	0.0000	0.80	486.2500	1.88	4.2149	4.01	3.8048
1.610	669.7430	0.0000	0.0000	0.0000	0.85	495.0280	1.91	4.6421	4.03	3.4126
1.710	635.8137	0.0000	0.0000	0.0000	0.91	487.5040	1.93	5.0853	4.06	3.0389
1.810	606.6909	0.0000	0.0000	0.0000	1.00	444.5570	1.96	5.5433	4.09	2.6842
1.910	582.4056	0.0000	0.0000	0.0000	1.05	412.9820	1.99	6.0148	4.11	2.3486
2.010	562.7629	0.0000	0.0000	0.0000	1.10	383.7440	2.01	6.4981	4.14	2.0324
2.110	547.3209	0.0000	0.0000	0.0000	1.15	366.0520	2.04	6.9915	4.16	1.7355
2.210	535.3706	0.0000	0.0000	0.0000	1.18	378.4010	2.06	7.4930	4.18	1.4576
2.310	525.8385	0.0000	0.0000	0.0000	1.20	539.9320	2.09	8.0005	4.21	1.1985
2.410	516.5085	0.0000	0.0000	0.0000	1.25	366.5280	2.11	8.5120	4.24	0.9578
2.510	484.1980	0.0000	0.0000	0.0000	1.30	276.4010	2.13	9.0250	4.26	0.7350
2.610	523.6514	0.0000	0.0000	0.0000	1.40	184.6590	2.16	9.5375	4.28	0.5294
2.710	512.2599	0.0000	0.0000	0.0000	1.50	148.8900	2.18	10.0469	4.31	0.3406
2.910	500.5668	0.1620	0.0000	0.0000	1.60	132.6990	2.21	10.5511	4.34	0.1678
3.010	483.8689	0.1643	0.0000	0.0000	1.70	125.6870	2.23	11.0477	4.36	0.0103
3.210	459.2613	0.6173	0.0000	0.0000	1.80	123.9960	2.26	11.5346		
3.310	447.2842	1.1332	0.0000	0.0000	1.90	125.6700	2.29	12.0098		
3.510	426.7816	2.3055	0.0000	0.0000	2.00	129.4350	2.31	12.4714		
3.610	418.3335	2.8065	0.0000	0.0000	2.10	134.3000	2.34	12.9175		
3.810	403.8153	3.5517	0.0000	0.0000	2.19	138.9460	2.36	13.3468		
3.910	397.2076	3.8193	0.0000	0.0000	2.30	144.2880	2.38	13.7577		
4.110	384.3365	4.2218	0.0000	0.0000	2.40	148.3820	2.41	14.1493		
4.210	377.8509	4.3823	0.0000	0.0000	2.50	151.4310	2.43	14.5205		
4.410	364.5327	4.6701	0.0000	0.0000	2.60	153.1350	2.46	14.8705		
4.510	357.6910	4.8120	0.0000	0.0000	2.70	153.8170	2.48	15.1990		
4.710	343.7649	5.1199	0.0000	0.0000	2.80	153.5780	2.51	15.5056		
4.810	336.7680	5.2949	0.0000	0.0000	2.90	155.0680	2.54	15.7901		
5.010	322.9796	5.7031	0.0000	0.0000	3.00	136.9140	2.56	16.0527		
5.110	316.3087	5.9397	0.0000	0.0000	3.20	131.3830	2.59	16.2934		
5.310	303.6924	6.4717	0.0000	0.0000	3.40	119.5240	2.61	16.5127		
5.410	297.6961	6.7555	0.0000	0.0000	3.50	114.2200	2.63	16.7110		
5.610	288.4262	7.2952	0.0000	0.0000	3.60	110.6100	2.66	16.8890		
5.710	282.4692	7.5121	2.1317	0.0000	3.70	109.4570	2.68	17.0472		
5.810	279.0839	7.6589	1.4524	0.0000	3.80	111.8530	2.71	17.1864		
5.910	275.5477	7.7717	1.6437	0.0000	3.90	119.5670	2.73	17.3074		
6.010	270.8025	7.8790	1.7416	0.0000	4.00	133.5590	2.76	17.4111		
6.110	273.2562	8.0102	1.8284	0.0000	4.05	140.1370	2.79	17.4984		
6.210	268.4856	8.1927	1.9395	0.0000	4.10	141.5020	2.81	17.5701		
6.310	264.1357	8.4342	2.1111	0.0000	4.15	145.8860	2.84	17.6271		
6.410	258.4442	8.6875	2.3607	0.0000	4.20	136.4740	2.86	17.6705		
6.510	251.3322	8.8143	2.7210	0.0000	4.22	132.2720	2.88	17.7010		
6.610	243.5747	8.7882	3.1683	0.0000	4.25	120.3990	2.91	17.7196		
6.710	236.2838	8.6067	3.5371	0.0000	4.28	102.1640	2.93	17.7272		
6.810	230.0665	8.3091	3.7800	0.0000	4.30	88.4482	2.93	17.7272		
6.910	225.1128	7.9491	3.9316	0.0000	4.32	75.6414	2.96	17.7196		
7.010	221.4064	7.5707	4.0305	0.0000	4.35	61.1426	2.98	17.7010		
7.110	218.8328	7.2010	4.1050	0.0000	4.38	52.9656	3.01	17.6705		
7.210	217.2490	6.8545	4.1725	0.0000	4.40	50.1612	3.04	17.6271		
7.310	216.5871	6.5379	4.2431	0.0000	4.50	48.5057	3.06	17.5701		
7.410	217.1682	6.2546	4.3229	0.0000	4.60	50.5447	3.09	17.4984		
7.510	222.2243	5.9887	4.4097	0.0000	4.80	53.2614	3.11	17.4111		
7.610	255.9595	4.9796	4.0128	0.0000	5.00	54.7982	3.13	17.3074		
7.710	220.3991	5.1341	4.2830	0.0000	5.20	55.9350	3.16	17.1864		
7.810	216.8351	5.0570	4.4498	0.0000	5.40	56.8581	3.18	17.0472		
7.910	216.4358	4.9003	4.5602	0.0000	5.60	57.2544	3.21	16.8890		
8.010	216.5021	4.7318	4.6621	0.0000	5.80	63.3500	3.23	16.7110		
8.110	214.5247	4.5573	4.7790	0.0000	6.00	55.5656	3.26	16.5127		
8.210	217.9746	4.4112	4.8935	0.0000	6.30	47.1333	3.29	16.2934		
8.310	218.0792	4.2531	5.0678	0.0000	6.60	45.0039	3.31	16.0527		
8.410	218.2221	4.0937	5.3612	0.0217	6.80	37.5633	3.34	15.7901		
8.510	218.2804	3.9313	6.0451	0.0839	7.00	36.4323	3.36	15.5056		
8.610	218.5848	3.7854	7.4958	0.1658	7.50	48.5773	3.38	15.1990		
8.710	218.9885	3.6701	6.9975	0.2336	8.00	53.2194	3.41	14.8705		
8.810	218.7214	3.5671	6.3863	0.2832	8.50	53.8344	3.43	14.5205		
8.910	218.2882	3.4694	6.2656	0.3278	9.00	48.0363	3.48	13.7577		
9.010	217.7033	3.3813	6.2923	0.3729	9.50	41.2731	3.51	13.3468		
9.110	216.9169	3.3103	6.3470	0.4192	10.00	56.8152	3.54	12.9175		
9.210	215.8539	3.2669	6.3937	0.4653			3.56	12.4714		
9.310	214.2592	3.2650	6.4805	0.5097			3.59	12.0098		
9.410	211.1859	3.3209	6.8876	0.5510			3.61	11.5346		
9.510	210.5804	3.4478	6.5011	0.5888			3.63	11.0477		

TABLE VII: Data on the electron scattering cross sections for CF_2 for selected energy points. Energies (E) are given in eV; cross sections are given in 10^{-21} m^2. The electronic archive presents the same data for 400 energy points. Key:
IEXS - integral alstic scattering cross section; EXCM - excitation to the first excited metastable $^3B_1$ state;
EXSB - excitation to the bound and radiative $^1B_1$ state; EXSO - excitation to other dissociative $^3A_2$, $^1A_2$ and $^3B_2$ states;
MTXS - momentum transfer cross section; DEA - estimated dissociative attachment cross section.

E	IEXS	EXCM	EXSB	EXSO	E	MTXS	E	DEA
0.110	353.8716	0.0000	0.0000	0.0000	0.12	284.3787	0.54	3.4609
0.210	228.5882	0.0000	0.0000	0.0000	0.15	267.3979	0.56	4.9342
0.310	182.7474	0.0000	0.0000	0.0000	0.18	257.1102	0.58	6.8380
0.410	159.4868	0.0000	0.0000	0.0000	0.20	252.4128	0.61	9.3229
0.510	146.5805	0.0000	0.0000	0.0000	0.22	248.8636	0.63	12.6073
0.610	141.4606	0.0000	0.0000	0.0000	0.25	245.0588	0.66	17.0147
0.710	149.7661	0.0000	0.0000	0.0000	0.28	242.5394	0.69	23.0339
0.810	208.8477	0.0000	0.0000	0.0000	0.30	241.3866	0.71	31.4168
0.910	294.7711	0.0000	0.0000	0.0000	0.32	240.5732	0.74	43.3335
1.010	183.0762	0.0000	0.0000	0.0000	0.35	239.8948	0.76	60.5933
1.110	139.6836	0.0000	0.0000	0.0000	0.38	239.7939	0.79	85.8479
1.210	122.7824	0.0000	0.0000	0.0000	0.40	240.0311	0.81	122.2926
1.310	113.7788	0.0000	0.0000	0.0000	0.42	240.5149	0.83	171.1748
1.410	107.8898	0.0000	0.0000	0.0000	0.45	241.7319	0.86	224.3300
1.510	103.5136	0.0000	0.0000	0.0000	0.48	243.6127	0.88	257.4859
1.610	99.9867	0.0000	0.0000	0.0000	0.50	245.2977	0.91	249.2274
1.710	96.9892	0.0000	0.0000	0.0000	0.52	247.3888	0.94	210.0358
1.810	94.3482	0.0000	0.0000	0.0000	0.55	251.4449	0.96	164.8515
1.910	91.9618	0.0000	0.0000	0.0000	0.58	256.9021	0.99	126.9306
2.010	89.7654	0.0000	0.0000	0.0000	0.60	261.5455	1.01	98.4208
2.110	87.7146	0.0000	0.0000	0.0000	0.62	267.2125	1.03	77.6137
2.210	85.7750	0.0000	0.0000	0.0000	0.65	278.2098	1.06	62.3859
2.310	83.9134	0.0000	0.0000	0.0000	0.68	293.3366	1.09	51.0704
2.410	82.0741	0.0000	0.0000	0.0000	0.70	306.6459	1.11	42.4997
2.510	79.9085	1.9401	0.0000	0.0000	0.72	323.3961	1.13	35.8801
2.610	78.5771	4.1955	0.0000	0.0000	0.75	357.4202	1.16	30.6722
2.710	77.3263	5.1657	0.0000	0.0000	0.78	406.3732	1.18	26.5054
2.810	76.1371	5.7443	0.0000	0.0000	0.80	449.5361	1.21	23.1202
2.910	75.0041	6.1178	0.0000	0.0000	0.82	500.7407	1.24	20.3323
3.010	73.9243	6.3666	0.0000	0.0000	0.85	578.0835	1.26	18.0080
3.110	72.8956	6.5339	0.0000	0.0000	0.88	604.3552	1.28	16.0489
3.210	71.9164	6.6462	0.0000	0.0000	0.90	567.2395	1.31	14.3811
3.310	70.9853	6.7208	0.0000	0.0000	0.92	497.5880	1.34	12.9487
3.410	70.1006	6.7696	0.0000	0.0000	0.95	385.9371	1.36	11.7085
3.510	69.2610	6.8011	0.0000	0.0000	0.98	303.4513	1.38	10.6268
3.610	68.4650	6.8216	0.0000	0.0000	1.00	265.9206	1.41	9.6770
3.710	67.7111	6.8358	0.0000	0.0000	1.05	211.1838	1.43	8.8378
3.810	66.9975	6.8475	0.0000	0.0000	1.10	185.2536	1.46	8.0922
3.910	66.3226	6.8600	0.0000	0.0000	1.20	163.4235	1.49	7.4262
4.010	65.6847	6.8759	0.0000	0.0000	1.30	154.2781	1.51	6.8285
4.210	64.5122	6.9280	0.0000	0.0000	1.50	144.8399		
4.310	63.9738	6.9689	0.0000	0.0000	1.60	141.4441		
4.510	62.9830	7.0930	0.0000	0.0000	1.80	135.5656		
4.610	62.5266	7.1815	0.0000	0.0000	1.90	132.9141		
4.810	61.6819	7.4254	0.0000	0.0000	2.10	128.0526		
5.010	60.9152	7.7783	0.0000	0.0000	2.30	123.7326		
5.210	60.2105	8.2624	0.0000	0.0000	2.50	119.9931		
5.310	59.8752	8.5613	0.0000	0.0000	2.60	118.2275		
5.510	59.2498	9.1961	0.2671	0.0000	2.80	115.1308		
5.610	58.9691	9.4598	0.5196	0.0000	2.90	113.7800		
5.710	58.6899	9.7118	0.7774	0.0000	3.00	112.5529		
5.810	58.4134	9.9324	1.0335	0.0000	3.10	111.4434		
5.910	58.1402	10.1061	1.2829	0.0000	3.20	110.4473		
6.010	57.8708	10.2217	1.5231	0.0000	3.40	108.7766		
6.210	57.3452	10.2583	1.9717	0.0000	3.80	106.6117		
6.310	57.0897	10.1823	2.1798	0.0000	4.00	106.0660		
6.510	56.5942	9.8772	2.5657	0.0000	4.40	105.9498		
6.610	56.3540	9.6685	2.7451	0.0000	4.60	106.3737		
6.710	56.1184	9.4357	2.9165	0.0000	4.80	107.1415		
6.910	55.6598	8.9326	3.2389	0.0000	5.20	109.9469		
7.010	55.4358	8.6757	3.3914	0.0000	5.40	112.1134		
7.210	54.9964	8.1736	3.6820	0.0000	5.80	121.1412		
7.310	54.7803	7.9337	3.8211	0.0000	6.00	129.4506		
7.410	54.5665	7.7035	3.9566	0.0000	6.20	137.3980		
7.610	54.1446	7.2744	4.2176	0.0000	6.40	135.8350		
7.710	53.9365	7.0760	4.3435	0.0000	6.50	133.4048		
7.910	53.5268	6.7105	4.5865	0.0000	6.65	136.8174		
8.010	53.3255	6.5427	4.7037	0.0000	6.70	140.7393		
8.210	52.9318	6.2347	4.9294	0.0000	6.80	145.4486		
8.410	52.5524	5.9602	5.1436	0.0000	6.90	128.3499		
8.510	52.3694	5.8343	5.2463	0.0000	6.95	117.0814		
8.710	52.0191	5.6028	5.4432	0.0000	7.10	99.0641		
8.810	51.8530	5.4963	5.5375	0.0000	7.20	94.9494		
9.010	51.5417	5.2982	5.7182	0.0000	8.20	89.8992		
9.110	51.3964	5.2025	5.8063	0.0047	8.50	89.6317		
9.210	51.2590	5.1105	5.8887	0.0197	8.80	89.4674		
9.310	51.1310	5.0250	5.9700	0.0354	9.00	89.4246		
9.410	51.0135	4.9460	6.0489	0.0508	9.20	89.4474		
9.410	51.0135	4.9460	6.0489	0.0508	9.20	89.4474		
9.510	50.9072	4.8728	6.1254	0.0653	9.50	89.6196		
9.610	50.8123	4.8045	6.1996	0.0819	9.80	89.9676		
9.710	50.7296	4.7407	6.2716	0.0963	10.00	90.2975		

TABLE VIII: Data on the electron scattering cross sections for CF_3 for selected energy points. Energies (E) are given in eV; cross sections are given in 10^{-21} m^2. The electronic archive presents the same data for 400 energy points. Key:
IEXS - integral alstic scattering cross section; EXC1 - excitation to the first excited A $^2A_2$ state;
EXS2 - excitation to the second excited B ^{2}E state; EXS3 - excitation to the third excited 2 ^{2}E state;
MTXS - momentum transfer cross section.

E	IEXS	EXCM	EXSB	EXSO	E	MTXS
0.110	1554.5261	0.0000	0.0000	0.0000	0.05	3101.3986
0.210	1015.3164	0.0000	0.0000	0.0000	0.10	2508.6964
0.310	800.8319	0.0000	0.0000	0.0000	0.15	2243.2498
0.410	680.7397	0.0000	0.0000	0.0000	0.20	2064.3855
0.610	545.9769	0.0000	0.0000	0.0000	0.30	1808.0135
0.710	503.4147	0.0000	0.0000	0.0000	0.35	1708.5579
0.810	469.8514	0.0000	0.0000	0.0000	0.40	1621.2515
1.010	419.8900	0.0000	0.0000	0.0000	0.50	1473.8914
1.110	400.6529	0.0000	0.0000	0.0000	0.55	1410.8940
1.210	384.0807	0.0000	0.0000	0.0000	0.60	1353.6554
1.410	356.8257	0.0000	0.0000	0.0000	0.70	1253.5653
1.510	345.4166	0.0000	0.0000	0.0000	0.75	1209.5944
1.610	335.1444	0.0000	0.0000	0.0000	0.80	1169.0578
1.810	317.3100	0.0000	0.0000	0.0000	0.90	1096.8330
1.910	309.4867	0.0000	0.0000	0.0000	0.95	1064.5344
2.110	295.5581	0.0000	0.0000	0.0000	1.10	979.9779
2.210	289.3161	0.0000	0.0000	0.0000	1.20	932.0004
2.410	278.0213	0.0000	0.0000	0.0000	1.40	851.1462
2.510	272.8916	0.0000	0.0000	0.0000	1.50	816.6578
2.610	268.0659	0.0000	0.0000	0.0000	1.60	785.3310
2.810	259.2303	0.0000	0.0000	0.0000	1.80	730.4621
2.910	255.1809	0.0000	0.0000	0.0000	1.90	706.2763
3.110	247.7387	0.0000	0.0000	0.0000	2.10	663.2246
3.210	244.3197	0.0000	0.0000	0.0000	2.20	644.0072
3.310	241.0870	0.0000	0.0000	0.0000	2.30	626.1432
3.510	235.1415	0.0000	0.0000	0.0000	2.50	594.0355
3.710	229.8320	0.0000	0.0000	0.0000	2.70	566.1666
3.810	227.3964	0.0000	0.0000	0.0000	2.75	559.8018
3.910	225.0975	0.0000	0.0000	0.0000	2.80	568.7307
4.010	222.9286	0.0000	0.0000	0.0000	2.85	547.6783
4.210	218.9554	0.0000	0.0000	0.0000	3.00	527.5409
4.310	217.1387	0.0000	0.0000	0.0000	3.10	520.9320
4.510	213.8160	0.0000	0.0000	0.0000	3.30	502.7043
4.610	212.2986	0.0000	0.0000	0.0000	3.40	494.5261
4.810	209.5245	0.0000	0.0000	0.0000	3.60	479.8417
4.910	208.2574	0.0000	0.0000	0.0000	3.70	473.2624
5.010	207.0637	0.0000	0.0000	0.0000	3.80	467.1440
5.210	204.8773	0.0000	0.0000	0.0000	4.00	453.6261
5.310	203.8756	0.0000	0.0000	0.0000	4.20	446.6361
5.510	202.0341	0.0000	0.0000	0.0000	4.60	431.0631
5.610	201.1863	0.0000	0.0000	0.0000	4.80	424.6141
5.710	200.3822	0.0000	0.0000	0.0000	5.00	418.8293
5.810	199.6181	0.0000	0.0000	0.0000	5.20	413.5699
5.910	198.8907	0.0000	0.0000	0.0000	5.40	408.7229
6.010	198.1967	0.0000	0.0000	0.0000	5.60	404.1972
6.110	197.5330	0.0000	0.0000	0.0000	5.80	399.9222
6.210	196.8966	0.0000	0.0000	0.0000	6.00	395.8433
6.310	196.2846	0.0000	0.0000	0.0000	6.20	391.9163
6.410	195.6944	0.0000	0.0000	0.0000	6.40	388.1049
6.510	195.1235	0.0000	0.0000	0.0000	6.50	384.6619
6.610	194.5693	0.0000	0.0000	0.0000	6.80	380.7091
6.710	194.0297	0.0000	0.0000	0.0000	7.00	377.0752
6.810	193.5026	0.0000	0.0000	0.0000	7.20	373.4585
6.910	192.9859	0.0000	0.0000	0.0000	7.50	368.0372
7.010	192.4781	0.0000	0.0000	0.0000	7.80	362.6859
7.110	191.9776	0.0000	0.0000	0.0000	8.00	359.0452
7.210	191.4829	0.0000	0.0000	0.0000	8.20	355.4540
7.310	190.9930	0.0000	0.0000	0.0000	8.50	350.1859
7.410	190.5069	0.0000	0.0000	0.0000	8.80	345.1753
7.510	190.0239	0.0000	0.0000	0.0000	9.00	342.0567
7.610	189.5436	0.0000	0.0000	0.0000	9.20	340.0155
7.710	189.0656	0.0000	0.0000	0.0000	9.50	335.5925
7.810	188.5898	0.0000	0.0000	0.0000	9.80	329.2728
7.910	188.1152	0.0019	0.0000	0.0000	10.00	339.1812
8.010	187.6450	0.0085	0.0000	0.0000		
8.110	187.1782	0.0151	0.0000	0.0000		
8.210	186.7160	0.0217	0.0000	0.0000		
8.310	186.2595	0.0285	0.0000	0.0000		
8.410	185.8099	0.0354	0.0000	0.0000		
8.510	185.3683	0.0424	0.0000	0.0000		
8.610	184.9359	0.0495	0.0000	0.0000		
8.710	184.5094	0.0569	0.0097	0.0000		
8.810	184.0901	0.0650	0.0284	0.0000		
8.910	183.6853	0.0745	0.0521	0.0000		
9.010	183.2954	0.0873	0.0765	0.0000		
9.110	182.9129	0.1095	0.1046	0.0000		
9.210	182.5194	0.1651	0.1446	0.0000		
9.310	182.1125	0.3208	0.2098	0.0000		
9.410	181.8618	0.3615	0.2721	0.0000		
9.510	181.6790	0.2714	0.3684	0.0000		
9.610	181.3324	0.3158	0.6487	0.0000		
9.710	181.5429	0.4110	0.6336	0.0000		
9.810	181.5669	0.4008	0.3443	0.0337		
9.910	181.5375	0.3823	0.3243	0.0519		